

Copyright
by
Raul Olvera
2019

**The Thesis Committee for Raul Olvera
Certifies that this is the approved version of the following Thesis:**

**Early-Age Shrinkage of Alkali-Activated Class F Fly Ash and Portland
Cement for Long-term Oil Well Zonal Isolation Control**

**APPROVED BY
SUPERVISING COMMITTEE:**

Maria G. Juenger, Supervisor

Eric van Oort, Co-Supervisor

Parth Panchmatia

**Early-Age Shrinkage of Alkali-Activated Class F Fly Ash and Portland
Cement for Long-term Oil Well Zonal Isolation Control**

by

Raul Olvera

Thesis

Presented to the Faculty of the Graduate School of

The University of Texas at Austin

in Partial Fulfillment

of the Requirements

for the Degree of

Master of Science in Engineering

The University of Texas at Austin

May 2019

Dedication

Dedicated to my parents, Raul and Maria, for giving me all of they could and more.

Acknowledgements

First and foremost, I would like to thank Dr. Parth Panchmatia for his guidance, expertise and commitment to the success of this project. You helped jumpstart this project when I knew nothing about oil wells and have always been there for support.

I would like to thank my advisers, Dr. Maria Juenger and Dr. Eric van Oort, for their leadership and guidance on this project. Dr. Juenger, thank you for helping grow my passion and interest in materials since my undergraduate years. Your positive attitude and encouragement at all times always paved the way forward. Dr. van Oort, thank you for allowing me to join such a strong research team and for introducing me to the petroleum industry. It has been a pleasure to learn from a world-class drilling engineer who always seems two steps ahead of everyone else.

I would like to acknowledge the CODA consortium sponsors for providing the research funding for this project along with their technical expertise along the way. Many thanks to Mike Rung, William Mickelson, and Reed Mickelson for their support with all of the equipment servicing and monitoring of experiments.

I would also like to thank UT ASCE and the UT Concrete Canoe team for getting me excited about my degree and for helping me find my area of interest in my first year at UT. To all the people at 18B, thank you for making the lab a fun place to work and always being willing to lend a hand, showing me how to run an experiment or collecting data. A special thanks to Saif Al-Shmaisani, for being here year after year and helping make research quite memorable.

Lastly, I would like to thank my family for being there through all the highs and lows. Thank you for always being caring, supportive, and giving me the opportunity to not

only pursue my dreams, but also encouraging me to dream bigger and bigger. Mom and Dad, you both continue to be my greatest role models and I could not be prouder to be your son. We did it!

Abstract

Early-Age Shrinkage of Alkali-Activated Class F Fly Ash and Portland Cement for Long-term Oil Well Zonal Isolation Control

Raul Olvera M.S.E.

The University of Texas at Austin, 2019

Supervisor: Maria Juenger, Eric van Oort

Volumetric changes due to shrinkage occur during the hydration/polymerization process of ordinary portland cement (OPC) and alkali-activated Class F fly ash systems. If not accounted for in the design of structures, especially those at elevated temperature and pressure conditions, shrinkage can develop internal stresses, which could generate micro-cracking. Specifically in oil and gas wells, shrinkage can compromise the hydraulic annular and result in loss of zonal isolation.

This thesis compares the early-age shrinkage behavior of Class H OPC, sodium hydroxide-activated Class F fly ash (geopolymer), and geopolymer-hybrid (geopolymers incorporating drilling mud) slurries with up to 20% (by volume) synthetic based mud (SBM) contamination cured at different temperatures and pressure conditions. A study into the effectiveness of zinc- and aluminum-based expansive agents for shrinkage mitigation is also presented. Shrinkage was recorded for specimens cured at temperatures between 23 - 80°C and up to 2000 psi confining pressure.

The results from testing indicate that A) temperature plays a major role in the shrinkage development of OPC and geopolymer slurries; B) pressure significantly increases OPC slurry shrinkage, but only minimally for geopolymers; C) addition of SBM increases shrinkage for OPC and geopolymer slurries; D) expansive agents can potentially counteract shrinkage in both OPC and geopolymer slurries. In addition, issues with shrinkage measurement at elevated temperature and pressure with current ASTM and API shrinkage tests are presented, along with a novel shrinkage measurement method avoiding these issues.

Table of Contents

List of Tables	xii
List of Figures	xiii
CHAPTER 1 : INTRODUCTION	1
1.1 Motivation.....	1
1.2 Objectives	3
1.3 Thesis Organization	3
CHAPTER 2 : BACKGROUND	5
2.1 Geopolymer: Definition and Terminology	5
2.2 Fly Ash-based Geopolymer	6
2.2.1 Aluminosilicate Source - Fly Ash.....	6
2.2.2 Alkali Solution	7
2.2.3 Polymerization Mechanism	8
2.4 Geopolymer Mix Design for Oil Well Cementing	9
2.4.1 Compressive Strength	10
2.4.2 Rheological Properties	12
2.4.3 Potential Industry Impact.....	15
2.5 Shrinkage	17
2.5.1 Chemical Shrinkage	17
2.5.2 Autogenous Shrinkage	18
2.5.3 Drying Shrinkage	18
2.5.4 Shrinkage Mitigation Techniques	19

CHAPTER 3 : MATERIALS AND METHODS	21
3.1 Raw Materials	21
3.1.1 Cementitious Materials	21
3.1.2 Activator Solution and Geopolymer Preparation.....	22
3.1.3 Synthetic-Base Mud (SBM).....	23
3.1.4 Expansive Agents.....	24
3.2 Experimental Methods.....	25
3.2.1 Capillary Tube Test.....	27
3.2.2 Membrane Test	29
3.2.3 Isothermal Calorimetry	31
3.2.4 Diaphragm Accumulator Test.....	32
3.2.5 Optical Microscope Imaging.....	36
CHAPTER 4 : RESULTS AND DISCUSSION	38
4.1 OPC and Geopolymer Shrinkage Behavior	38
4.2 Effects of SBM Contamination on the Shrinkage of OPC and Geopolymer Slurries	42
4.3 Heat of Hydration Comparison to Shrinkage	45
4.4 Effect of Expansive agents on OPC and Geopolymer Shrinkage Behavior	50
4.5 Shrinkage Testing at High Pressure High Temperature Conditions.....	54
4.5.1 Temperature Effects.....	55
4.5.2 Effects of Expansive Agents	60
4.5.2.1 Effect of Expansive Agents on OPC Slurries	60
4.5.2.2 Effect of Expansive Agents on Geopolymer Slurries	63
4.5.3 Effects of Elevated Pressure	66

4.6 Optical Microscope Imaging	70
CHAPTER 5 : CONCLUSIONS AND FUTURE WORK.....	74
5.1 Conclusions.....	75
5.2 Recommendations for Future Work	79
REFERENCES.....	81

List of Tables

Table 3.1: Oxide composition of Class F fly ash and Class H OPC employed in this study.....	22
Table 3.2: Properties of the SBM formulation used in this study.....	24
Table 3.3: Composition of zinc-based expansive agent.....	25
Table 3.4: Composition of aluminum-based expansive agent.	25

List of Figures

Figure 2.1: Ternary phase diagram showing OPC, blast furnace slag, fly ash, silica fume, and metakaolin composition. Reprinted with permission from Liu (2017).	7
Figure 2.2: Alkali activation process in hydroxide-based reactions. Adopted from Juenger, 2011.	9
Figure 2.3: Normalized compressive strength of OPC (P1S1) and geopolymer (G1S1) with SBM contamination at 24hours, 76.6°C (170°F) and 3000 psi. Reprinted with permission from Liu (2017).	11
Figure 2.4: Compressive strength of geopolymer (G1) and geopolymer hybrids at 20% (G1S1-20), 30% (G1S1-30), and 40% (G1S1-40) contamination at 76.6°C (170°F) and 3000 psi. Reprinted with permission from Liu (2017).	12
Figure 2.5: Rheological properties in (a) OPC slurries with 0% (P1), 5 % (P1S1-5), 10% (P1S-10), and 15% (P1S1-15)SBM contamination and.(b) geopolymers with 0-40% SBM contamination at 21°C (70°F). Reprinted with permission from Liu (2017).	14
Figure 2.6: Rheological properties of geopolymer (G1), geopolymer hybrids with 20% SBM contamination (G1S1-20), and OPC (P1-R) slurries at 21°C (70°F) and 51.6°C (125°F). Reprinted with permission from Liu (2017).	15
Figure 2.7: Estimated CO ₂ reduction with the use of geopolymers. Solid point are fly ash-based geopolymers while open circles are metakaolin-based geopolymers. Obtained from Duxon et al., 2007.	16
Figure 3.1: Capillary tube test setup employed in this study.	29

Figure 3.2: Membrane test setup used in this study.....	31
Figure 3.3: Diaphragm accumulator components. Obtained from the Accumulators, Inc. (diaphragm accumulator manufacturer) website (https://www.accumulators.com , 2019).....	35
Figure 3.4: Diaphragm accumulator set-up employed in this study.	36
Figure 3.5: Diaphragm accumulator sample after polishing.....	37
Figure 4.1: Chemical shrinkage in OPC and geopolymer slurries at 23°C and 50°C, measured using the capillary tube test.	41
Figure 4.2: Autogenous shrinkage of neat OPC and geopolymer slurries at 23°C, measured using the membrane test.	42
Figure 4.3: Chemical shrinkage of geopolymer slurries contaminated with SBM, measured using the capillary tube test.	44
Figure 4.4: Chemical shrinkage of OPC slurries contaminated with SBM, measured using the capillary tube test.....	45
Figure 4.5: Rate of heat release at 23°C, as measured by isothermal calorimetry.	48
Figure 4.6: Rate of heat release at 50°C, as measured by isothermal calorimetry.	48
Figure 4.7: Cumulative heat released by OPC and geopolymers at 23°C, measured using isothermal calorimetry.....	49
Figure 4.8: Cumulative heat released from OPC and geopolymer mixes at 50°C, measured using isothermal calorimetry.	49
Figure 4.9: Geopolymers with zinc-based expansive agents tested at 23°C and 50°C, measured using the capillary tube test. Positive values represent sample volume expansion; negative values correspond to shrinkage.	52

Figure 4.10: Geopolymers with aluminum-based expansive agents tested at 23°C and 50°C, measured using the capillary tube test. Positive values represent sample volume expansion; negative values correspond to shrinkage.....	53
Figure 4.11: OPC with zinc- and aluminum-based expansive agents tested at 23°C and 50°, measured using the capillary tube test. Positive values indicate sample expansion; negative values correspond to shrinkage.....	54
Figure 4.12: OPC shrinkage at 200 psi and 40°C or 80°C, measured using the diaphragm accumulator test.	59
Figure 4.13: Geopolymer shrinkage at 200 psi and 35°C, 40°C, or 80°C, measured using the diaphragm accumulator test.....	60
Figure 4.14: OPC shrinkage with zinc-based expansive agent at 200 psi and 40°C or 80°C, measured using the diaphragm accumulator test.	62
Figure 4.15: OPC shrinkage with 0.4% Aluminum expansive agent at 200 psi and 40°C or 80°C, measured using the diaphragm accumulator test.	63
Figure 4.16: Geopolymer shrinkage with zinc-based expansive agent at 40°C and 200 psi, measured using the diaphragm accumulator test.....	65
Figure 4.17: Geopolymer shrinkage with zinc-based expansive agent at 80°C and 200 psi, measured using the diaphragm accumulator test.....	65
Figure 4.18: OPC shrinkage with zinc-based expansive agent at 200 psi and 40°C or 80°C, measured using the diaphragm accumulator test.	66
Figure 4.19: OPC shrinkage at 2000 psi and 40°C, measured using the diaphragm accumulator test.	69
Figure 4.20: OPC shrinkage with zinc- and aluminum-based expansive agents at 2000 psi and 40°C, measured using the diaphragm accumulator test.	69

Figure 4.21: Geopolymer shrinkage at 2000 psi and 40°C, measured using the diaphragm accumulator test.	70
Figure 4.22: OPC sample tested at 40°C and 200 psi. Optical microscope images (b and c) taken at 0.8X magnification.	71
Figure 4.23: OPC samples with 1) 0.4% aluminum-based expansive agent at 40°C and 200 psi. 2) 0.4% aluminum-based expansive agent at 80°C and 200 psi. 3) 0.4% aluminum-based expansive agent at 40°C and 2000 psi. Optical microscope images (b and c) taken at 0.8X magnification.	72
Figure 4.24: OPC samples with 1) 0.09% zinc-based expansive agent at 40°C and 200 psi. 2) 0.09% zinc-based expansive agent at 80°C and 200 psi. 3) 0.09% zinc-based expansive agent at 40°C and 2000 psi. Optical microscope images (b and c) taken at 0.8X magnification.	73

CHAPTER 1 : INTRODUCTION

1.1 MOTIVATION

Advances in drilling technology and techniques over the last several decades have allowed for hydrocarbon operations in what were previously unreachable reservoirs. These advances have paved the way for progressive drilling operations in environments with narrow drilling margins and have resulted in the extended use of directional and horizontal drilling. While this may allow for greater production, it results in tighter margins of error leading to such issues as poor casing centralization, wellbore enlargements, and losses while cementing oil wells. These increase the risk of contamination of ordinary portland cement (OPC) slurries by non-aqueous fluids (NAFs), such as oil-based and synthetic based muds (OBM/SBM), which is detrimental to the strength and rheological properties of the cement (Aughenbaugh et al., 2014; Beach and Goins, 1957; Miranda et al., 2007). Any setbacks in these areas can potentially compromise zonal isolation of hydrocarbon-bearing formations and necessitate costly repairs.

In addition to issues relating to the contamination of OPC slurries with SBM/OBM, shrinkage, an inherent characteristic of OPC slurries (Kosmatka and Wilson, 2011; Powers, 1935; API 10B-5 / ISO 10426-5), has the potential to compromise zonal isolation. As the cement shrinks, it can develop internal stresses and/or forms a micro-annulus along the interface of the downhole rock formation and/or steel casing. If these internal stresses exceed the tensile strength of the slurry, cracking can occur, thus compromising the hydraulic annular or plug seal and promoting inter-zonal communication (API 10B-5 / ISO 10426-5).

To address the aforementioned issues, there is a need to develop alternatives to OPC slurries for cementing oil and gas wells, with more tolerance to contamination and less

asdfadsfasdfasdfasdf

shrinkage. Geopolymers, which are low calcium alkali-activated aluminosilicate materials, are currently used in a variety of construction applications and show promise as an oil and gas well cementing material. Research has shown that geopolymers and geopolymer-hybrids (geopolymers mixed with OBM/SBM) have the required strength, rheological properties, and pumpability to be suitable for primary cementing and lost circulation control applications (Liu et al., 2016 & 2017; Liu 2017). In addition to satisfying the strength and rheological requirements for oil well cements, geopolymers have proven to be more compatible with NAFs than OPC slurries, but more importantly, also show an ability to solidify NAFs. This property would allow for disposal of NAFs in situ, meaning the well operation would become more economical and environmentally friendly (Liu, 2017; Aughenbaugh et. al., 2014). Despite several instances of high performance in terms of strength, rheology, and other properties using geopolymers, the shrinkage behavior of geopolymers remains a topic of interest. Published studies on geopolymer shrinkage have shown contrasting results in testing, suggesting that geopolymer shrinkage merits further investigation, and starting materials, formulation, and curing regime will significantly affect shrinkage (Provis and van Deventer, 2014, Yong, 2010).

This study focused on characterizing the shrinkage behavior of geopolymer mixtures (designed following recommendations from Liu (2017) and Liu et al. (2016)) that show adequate/superior performance for oil well cementing applications compared to OPC. Specifically, this study evaluated the early-age shrinkage behavior of Class H OPC slurries compared to an 8M sodium hydroxide-activated Class F fly ash (referred in the following as geopolymer) slurry. The effects of temperature, pressure, and SBM contamination on the shrinkage behavior of both OPC and geopolymer slurries was considered, as well as possible shrinkage mitigation using expansive agents. These results

will help to further determine the adequacy for geopolymers to become the next generation of oil well cementing materials.

1.2 OBJECTIVES

The goal of this research study was to further the understanding of geopolymers and geopolymer-hybrids with respect to shrinkage and to continue to evaluate their suitability for oil-well cementing. The specific objectives and research questions for this study were as follows:

1. Characterize the magnitude of shrinkage in both geopolymers and OPC slurries using various testing methods.
2. Evaluate temperature effects on shrinkage from room temperature (23°C) up to 80°C.
3. Examine the effects of addition of SBM into geopolymer and OPC mixtures on the shrinkage behavior of those mixtures.
4. Evaluate the use of expansive agents for shrinkage mitigation of OPC and geopolymer formulations. Specifically, will the use of exothermic reacting zinc- and/or aluminum-based expansive agents provide shrinkage mitigation for geopolymers and/or OPC slurries?
5. Determine whether the current industry standards for shrinkage testing are adequate for proper shrinkage evaluation.

1.3 THESIS ORGANIZATION

The study presented in this thesis is broken down into five chapters. Chapter 2 provides an overview into the origins, terminology, and formulations of geopolymers. Previous studies demonstrating the advantages of geopolymers (over OPC) as an oil well

cement are summarized in Chapter 2. Furthermore, the literature on shrinkage mechanisms and measurement techniques for OPC slurries and how they might apply to geopolymer slurries are also discussed in Chapter 2. Chapter 3 provides a detailed description of the materials used during this study along with an explanation of the laboratory testing performed. Chapter 4 presents and compares the shrinkage behavior observed in OPC and geopolymer slurries with discussions on the mechanisms affecting the shrinkage behavior. Lastly, Chapter 5 highlights the key findings from this research and presents recommendations and suggestions for future work.

CHAPTER 2 : BACKGROUND

This chapter provides a brief description of the definitions and terminologies required to understand geopolymer formulations. In addition, a review of previous geopolymer work confirming the potential for geopolymer use in oil well operations is presented. Finally, a detailed description of the various types of shrinkage mechanisms experienced by cementitious materials (including geopolymers) is presented, coupled with an overview of existing shrinkage control methods.

2.1 GEOPOLYMER: DEFINITION AND TERMINOLOGY

The origins of cement date back to 7000 B.C. and its chemistry has been widely studied and optimized since then. Modern day construction demands OPC production on the order of 2.9 billion tons a year; therefore, making OPC concrete the second-most used commodity in the world behind water (Provis and van Deventer, 2014; Kostmatka and Wilson, 2015). In contrast, alkali-activated materials (AAMs) have only been studied for just over a century, after Kühl patented a hydroxide activated slag material in 1908 (Kühl, 1908). In its simplest form, an alkali-activated material involves the reaction of an alkaline solution with an alumina- and silica-rich precursor (Provis and van Deventer, 2014). Previous research on AAMs has provided promising results showing comparable and/or superior results to OPC mixtures in terms of strength and rheology, depending on the mixture design (Duxson et al., 2006; Duxson et al., 2008; Provis and van Deventer, 2014). Commonly used aluminosilicate precursors to produce AAMs include ground granulated blast furnace slag, fly ash, and metakaolin. Sodium or potassium-based hydroxide or silicate solutions are commonly used to activate these aluminosilicate precursors to produce AAMs (Somna, 2011, Duxson and Provis, 2008, Duxson et al., 2007, Chen and Brouwers, 2007).

This study focused on geopolymers, which are a subset of AAMs. The term geopolymers is used to describe AAMs that are composed of low calcium or calcium-free aluminosilicates as precursors (Juenger et al., 2011; Provis and van Deventer, 2014). Specifically, the geopolymer used in this study was a Class F fly ash activated by an 8M sodium hydroxide solution.

2.2 FLY ASH-BASED GEOPOLYMER

2.2.1 Aluminosilicate Source - Fly Ash

Fly ash is produced during the combustion of coal in power plants (Kosmatka, 2015). Fly ash is composed of the mineral impurities of the coal (e.g. clay, feldspar, quartz, etc.) that are fused during combustion and solidify into mostly glassy particles upon cooling. The particles are in fine powder form, and are collected from the exhaust gas using electrostatic precipitators. The chemical composition and properties of the fly ash depend on the type of coal used and the operating conditions of the power plant. Fly ashes are broadly categorized as either Class C or Class F based on the amount of silicon dioxide (SiO_2), aluminum oxide (Al_2O_3), and iron oxide (Fe_2O_3) present in them. According to ASTM C618-17, fly ashes with the sum of SiO_2 , Al_2O_3 , and Fe_2O_3 of 50-70% are classified as Class C, whereas fly ashes with a sum of SiO_2 , Al_2O_3 , and Fe_2O_3 greater than 70% are classified as Class F.

As previously stated, this study focused on the use of a low calcium Class F fly ash. Therefore, the resulting AAM can be classified as a geopolymer. Class F fly ashes are silica- and alumina-rich, but low are in lime content. Figure 2.1 illustrates the differences in the chemical composition of fly ash (both Class C and Class F) and other cementitious materials. The crystalline phases present in Class F fly ashes are quartz, mullite, hematite, and magnetite (Kosmatka, 2015; Hemmings and Berry, 1987). Low calcium fly ashes, like

the one used in this study, are not hydraulic (i.e. they do not react with water) and therefore need to be activated by an alkaline solution.

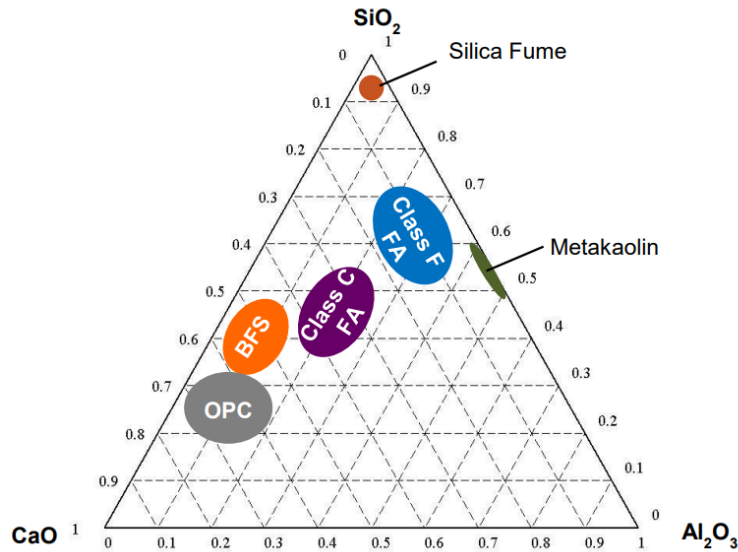


Figure 2.1: Ternary phase diagram showing OPC, blast furnace slag, fly ash, silica fume, and metakaolin composition. Reprinted with permission from Liu (2017).

2.2.2 Alkali Solution

For Class F fly ash to polymerize and form a three dimensional solid it must be activated with an alkaline solution. In this study, an 8M sodium hydroxide solution was used to activate the Class F fly ash. This decision was based on literature results confirming the efficacy of an 8M sodium hydroxide solution in activating Class F fly ash (Liu, 2017; Duxson et al., 2006, Provis and van Deventer, 2009) and adequate mechanical and rheological properties of the resulting geopolymer for oil well cementing (Liu, 2017, Liu et al., 2016).

2.2.3 Polymerization Mechanism

The activation mechanisms in AAMs are complex and depend on the solid precursor, alkali activator, and temperature. The specifics behind the process are still debated among researchers, but it is generally agreed that polymerization in AAMs takes place in two primary steps: dissolution and precipitation (Duxson et al., 2006; Juenger et al., 2011). When the alkaline solution is mixed with the aluminosilicate source, both silicate and aluminate ions (from the aluminosilicate source) begin to dissolve in the alkaline solution, in a process known as alkaline hydrolysis (Duxson et al., 2006). Precipitation of an aluminum-rich gel occurs as soon as critical concentrations of aluminate ions are reached in the solution. The composition of this gel evolves over time, through rearrangement and exchange of dissolved species as silicate and aluminate ions dissolve into the solution, resulting in a gel that is silicon-rich (Duxson et al., 2006; Duxson and Provis, 2008). Upon hardening, the gel forms a structure very similar to zeolites in which SiO_4 and AlO_4 are arranged in a tetrahedron and linked by a shared oxygen atom. When Class F fly ash is activated using NaOH, the end product includes two aluminosilicate gels, a N-A-S-(H) gel and C-A-S-(H) gel, where N is Na_2O , A is Al_2O_3 , S is SiO_2 , C is CaO , and H is water (Juenger et al., 2011; Fernandez-Jimenez et al., 2008; Davidovits, 1989; Duxson et al., 2007). Since the calcium content of the fly ash used in this study is very low, the reaction product would predominantly be N-A-S-(H). Figure 2.2 summarizes the polymerization process for geopolymers prepared using Class F fly ash and sodium hydroxide.

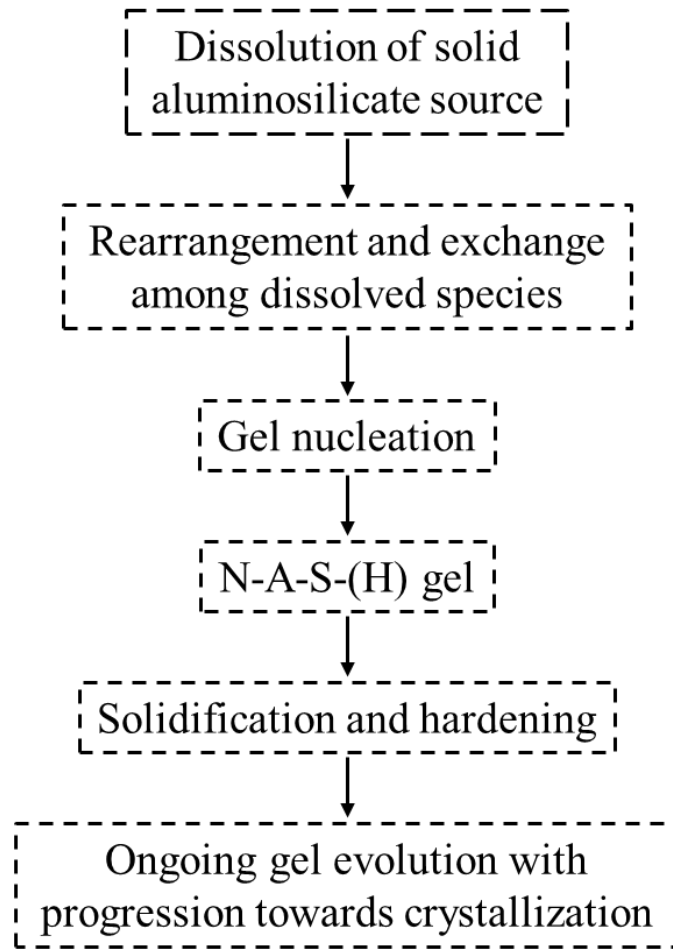


Figure 2.2: Alkali activation process in hydroxide-based reactions. Adopted from Juenger, 2011.

2.4 GEOPOLYMER MIX DESIGN FOR OIL WELL CEMENTING

As previously stated, the mixture designs for geopolymer and geopolymer- hybrids tested in this study were obtained from Liu (2017) and Liu et al. (2016). The following sections (2.4.1 – 2.4.3) summarize their findings for the geopolymer and geopolymer-hybrid systems prepared using Class F fly ash and 8M sodium hydroxide solution with respect to oil well cementing operations.

2.4.1 Compressive Strength

While OPC slurries typically meet the strength requirements for oil-well applications during laboratory testing, contamination with NAFs during real world operations can result in significant compressive strength loss. Liu (2017) demonstrated that 5% (by volume) contamination of OPC slurries with SBM resulted in 65% reduction in 1-day compressive strength when the samples were cured at 76.6°C (170°F) and 3000 psi. On the other hand, geopolymers prepared using Class F fly ash and 8M sodium hydroxide lost only 30% of their compressive strength when tested under the same conditions and contamination levels. Furthermore, the geopolymer samples maintained measurable compressive strength at up to 40% SBM (by volume) contamination, while the OPC slurry had no measurable strength at 30% SBM (by volume) contamination. These results, which are presented in Figure 2.3, demonstrate that geopolymers have better compatibility with SBM than OPC slurries.

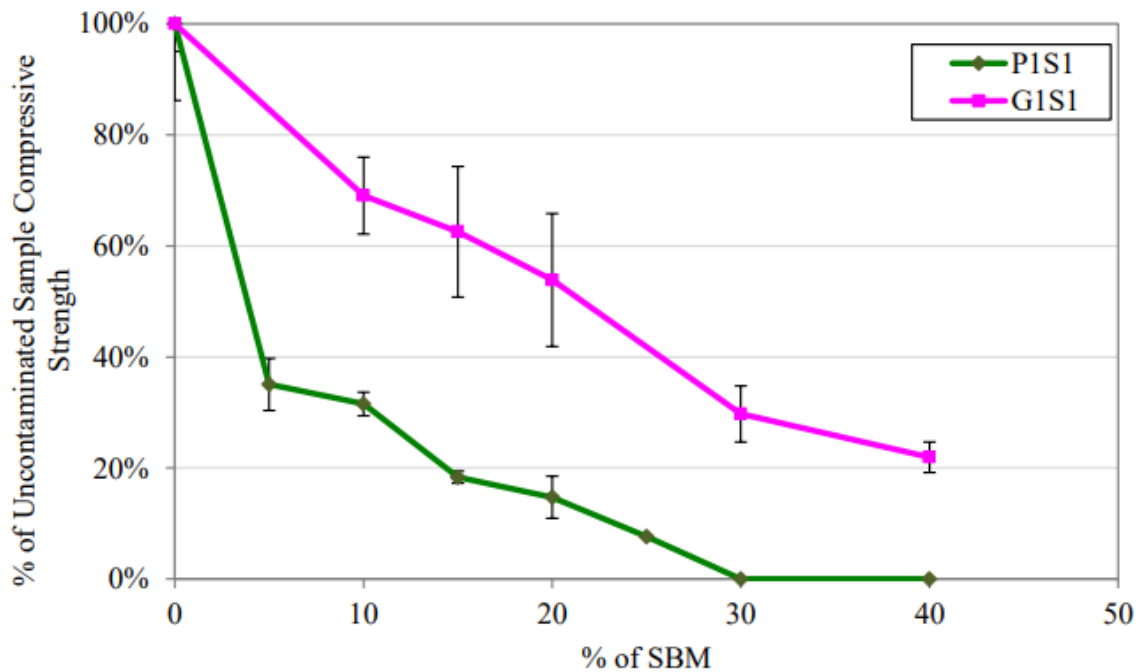


Figure 2.3: Normalized compressive strength of OPC (P1S1) and geopolymer (G1S1) with SBM contamination at 24hours, 76.6°C (170°F) and 3000 psi. Reprinted with permission from Liu (2017).

Figure 2.4 shows the compressive strength of geopolymer/geopolymer-hybrids with up to 40% (by volume) SBM contamination cured at 76.6°C (170°F) and 3000 psi. At higher levels of contamination, i.e. 30 and 40% (by volume), the compressive strengths reached were 1000 psi and 400 psi, respectively, after 14 days of curing. These strength values are appropriate for lost-circulation control applications in wells. In contrast, at lower contamination levels, i.e. 20% (by volume), the geopolymers/geopolymer-hybrids reached compressive strengths of over 2000 psi after 14 days of curing, which is suitable for most primary cementing applications (Liu, 2017).

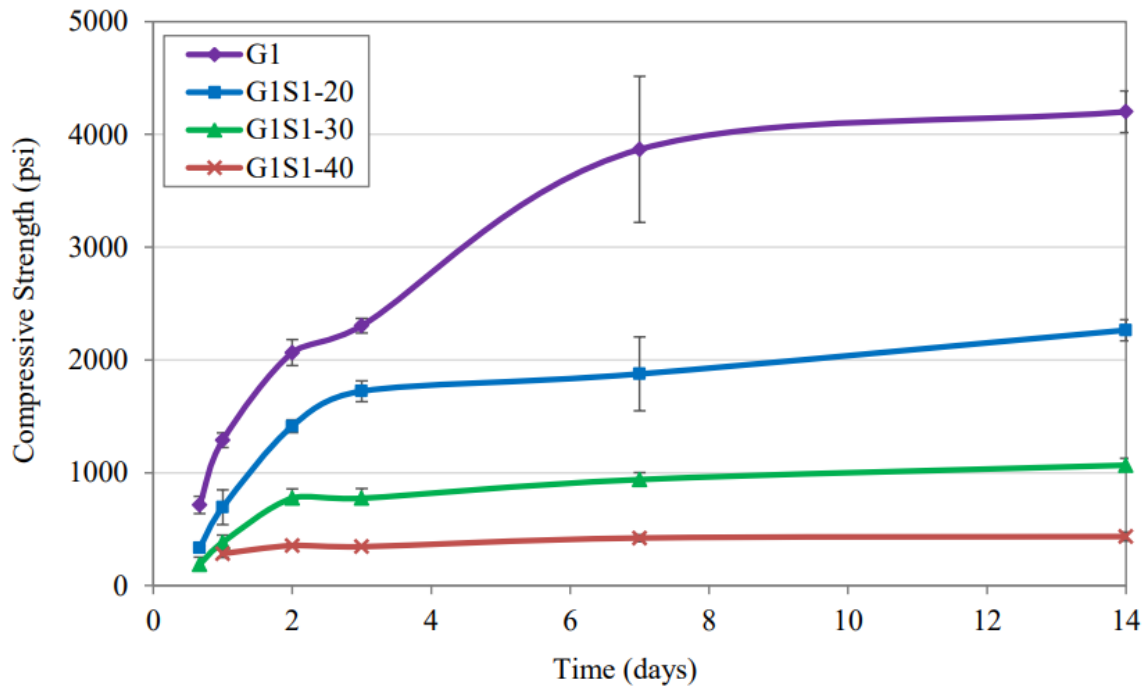


Figure 2.4: Compressive strength of geopolymer (G1) and geopolymer hybrids at 20% (G1S1-20), 30% (G1S1-30), and 40% (G1S1-40) contamination at 76.6°C (170°F) and 3000 psi. Reprinted with permission from Liu (2017).

2.4.2 Rheological Properties

Flowability is an important characteristic for oil well cement slurries. Traditional oil well cement slurries, which are prepared using Class H or G OPCs, have sufficiently low viscosity that makes them easy to pump downhole. However, upon contamination with NAFs during the displacement operations, viscosity increases at the leading edge of the cement slurry, potentially leading to excessive pumping pressure and fracturing (Enayatpour and van Oort, 2017; Liu, 2017). Liu (2017) confirmed that the viscosity of OPC slurries increased significantly due to contamination with SBM (Figure 2.5a).

In contrast, geopolymer slurries prepared using Class F fly ash and 8M sodium hydroxide experienced a reduction in viscosity when contaminated with SBM (geopolymer-hybrids). Neat geopolymer slurries prepared using Class F fly ash and 8M

sodium hydroxide are very stiff and therefore not pumpable. However, geopolymer-hybrid slurries with 30% and 40% (by volume) SBM had a similar viscosity to that of neat OPC slurry at 21°C (70°F). These results are presented in Figure 2.5b. Furthermore, when tested at an elevated temperature of 51.6°C (125°F), the viscosities of OPC slurries with and without SBM increased whereas the viscosities of geopolymer and geopolymer-hybrid slurries were reduced (Figure 2.6). This implies that geopolymer-hybrid systems could be easier to pump in real life scenarios than an OPC slurry that is contaminated during displacement.

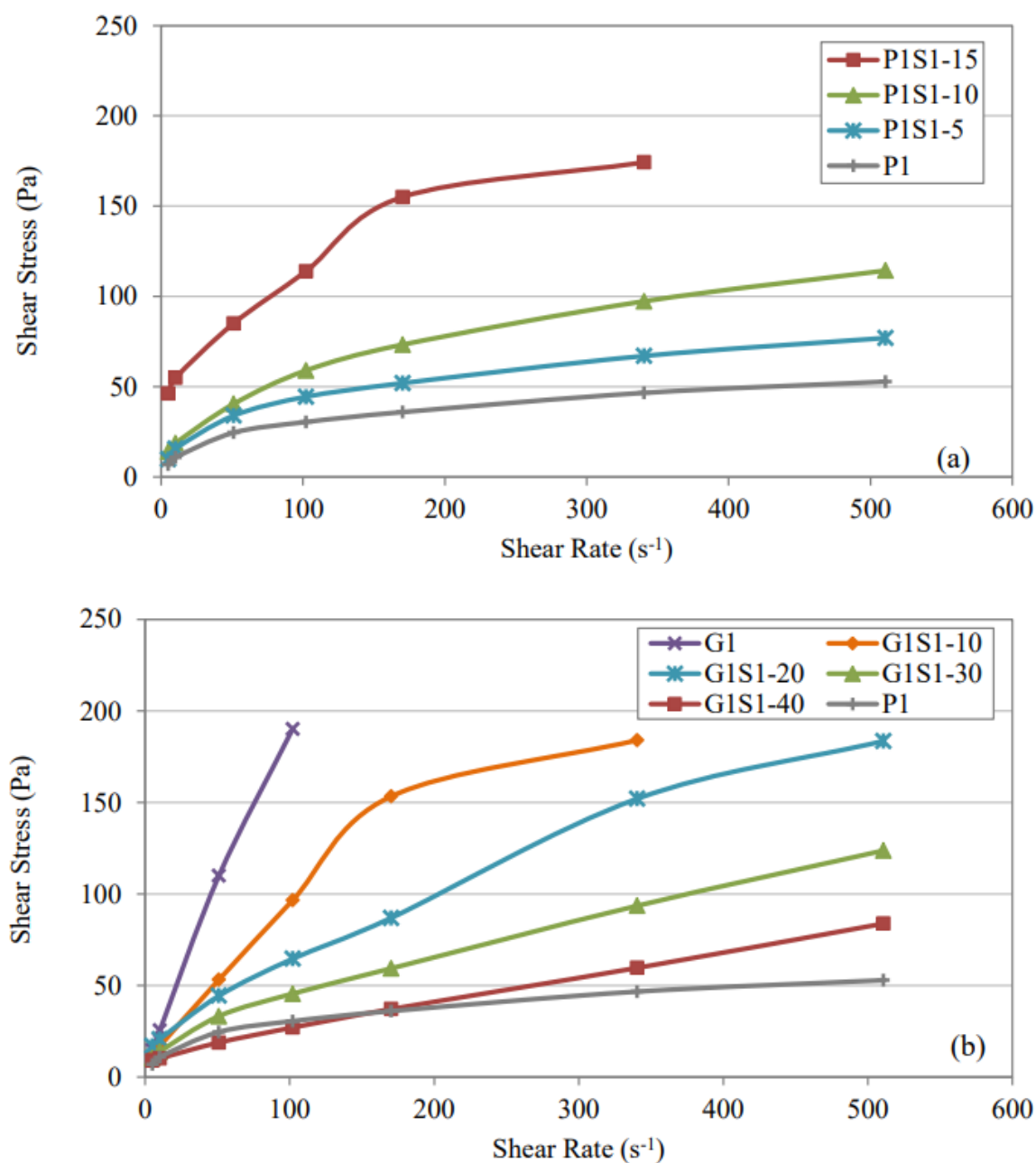


Figure 2.5: Rheological properties in (a) OPC slurries with 0% (P1), 5 % (P1S1-5), 10% (P1S1-10), and 15% (P1S1-15)SBM contamination and.(b) geopolymers with 0-40% SBM contamination at 21°C (70°F). Reprinted with permission from Liu (2017).

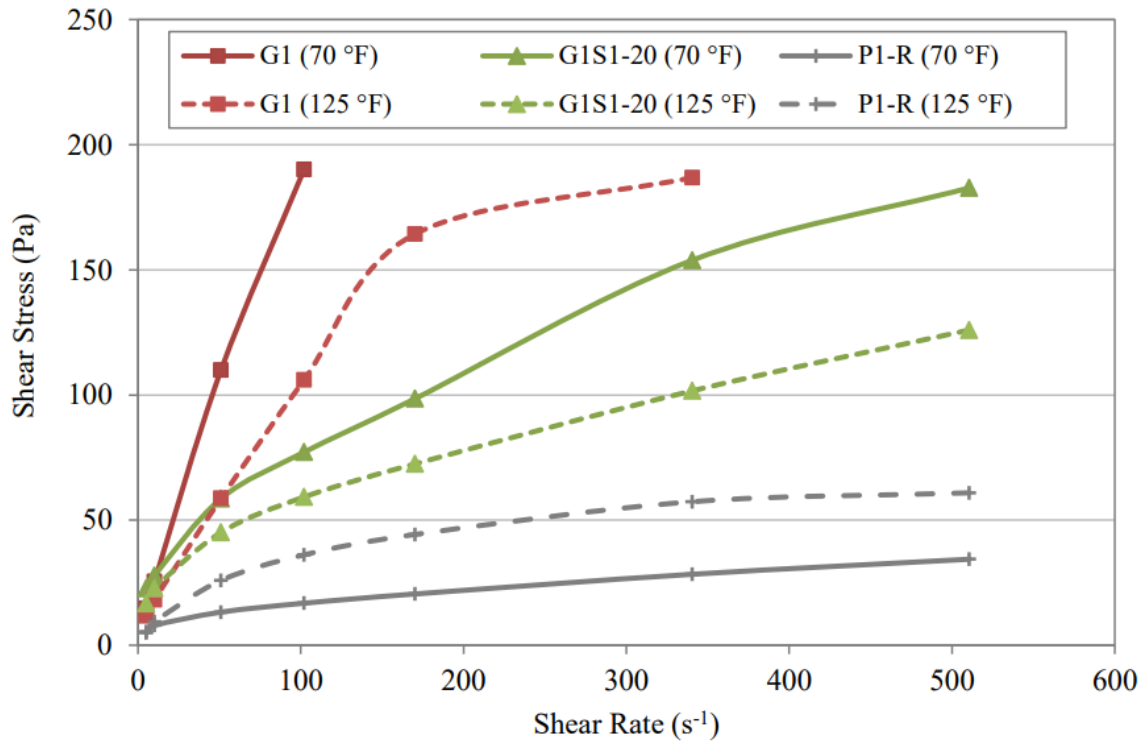


Figure 2.6: Rheological properties of geopolymer (G1), geopolymer hybrids with 20% SBM contamination (G1S1-20), and OPC (P1-R) slurries at 21°C (70°F) and 51.6°F (125°F). Reprinted with permission from Liu (2017).

2.4.3 Potential Industry Impact

The ability for geopolymers to have reduced viscosity and maintain strength despite contamination with SBM confirms that geopolymers have the potential to replace OPC for oil well cementing applications. In Liu (2017), additional data are provided to confirm that, while SBM type, fly ash source, seawater, and activator may alter material properties, they do not significantly change the properties and behavior previously discussed. Furthermore, geopolymer mixture designs can be optimized for specific oil well applications. The geopolymer's compatibility with NAFs would allow for superior zonal isolation and reduced risk of poor cementation as well as provide a means to dispose NAFs in-situ in an environmentally-friendly manner (Liu, 2017). Furthermore, replacing OPC with

geopolymers would help reduce the environmental footprint of oil well construction as the production of 1 ton of OPC releases approximately 0.90 tons of CO₂ (Duxon et al., 2007). Figure 2.7 shows the estimated reduction of CO₂ when geopolymers are used instead of OPC.

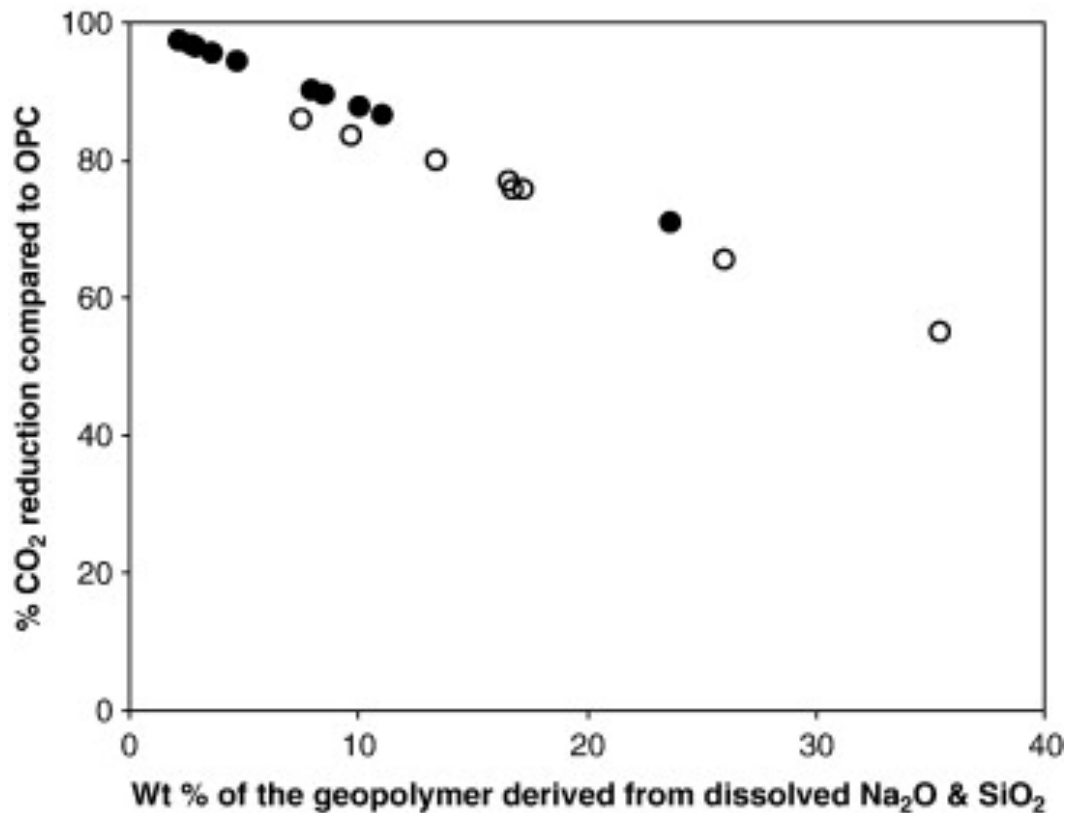


Figure 2.7: Estimated CO₂ reduction with the use of geopolymers. Solid point are fly ash-based geopolymers while open circles are metakaolin-based geopolymers. Obtained from Duxon et al., 2007.

Overall, geopolymers look like a prime candidate to replace OPC for oil well cementing applications. Not only do they appear to have the necessary properties and behavior to be successfully used as an oil well cement, they also have major environmental benefits, which would help the image of the oil well industry. Nevertheless, there are no

studies on OPC/geopolymers with SBM contamination in regard to shrinkage, which is critical to zonal isolation. Therefore, this study aims to characterize the shrinkage behavior of particular geopolymer formulations that have shown promising results for application in the oil well industry (i.e. geopolymers produced using Class F fly ash and 8M sodium hydroxide and geopolymer-SBM hybrids).

2.5 SHRINKAGE

After cement slurry placement, volume changes caused by changes in pore volume, pore pressure, or sample dimensions can lead the slurry to either shrink or expand. These changes in volume can lead to significant tensile stresses that can cause cracks. When taking place in an oil well, shrinkage has been known to lead to a micro-annulus along the interface with the rock formation and/or steel casing, causing interzonal communication and compromising the hydraulic annular or plug seal (API 10B-5). In the following sections, the main types of shrinkage mechanisms proposed in literature to explain shrinkage in OPC slurries, namely chemical shrinkage, autogenous shrinkage, and drying shrinkage are described.

2.5.1 Chemical Shrinkage

Chemical shrinkage refers to the absolute volume reduction that develops as the cement particles hydrate and arises because the volume of the hydration products is less than that of the reactants (Kosmatka and Wilson, 2011). During the initial plastic stage, the cement paste shrinks, but is still in a fluid-like state. Thus, no internal stresses are developed. Upon initial set, however, chemical shrinkage continues as cement hydrates, but with reduced ability for the cement matrix to deform; this shrinkage can result in the

development of internal stresses. If internal stresses become greater than the strength, shrinkage cracks may result.

2.5.2 Autogenous Shrinkage

Autogenous shrinkage refers to the visible dimension changes caused by cement hydration when there is a lack of internal water within the cement matrix. Once all external/free water has been consumed by cement for hydration, the remaining non-hydrated cement will pull water from its own pore structure to continue hydration. This self-desiccation process (i.e. consumption of its own pore water) will result in a uniform volume reduction in cement paste, which can lead to further internal stress development (Kosmatka and Wilson, 2011; Copeland and Bragg, 1955; Radlinska et al., 2008).

Chemical and autogenous shrinkage are measured in different ways because the former occurs when exposed to water, while the latter occurs in systems closed off from additional water. However, the occurrence of autogenous shrinkage is related to and driven by chemical shrinkage since the hydration of cement particles (and subsequent volume reduction) causes the lack of water in the cement matrix. After hardening, volume reduction is more constrained by the rigid cement paste, and thus autogenous shrinkage is reduced, while chemical shrinkage continues through ongoing cement hydration (Brooks, 2015).

2.5.3 Drying Shrinkage

Drying shrinkage refers to volumetric changes caused by moisture loss in the cement slurry due to the humidity and temperature of the surrounding environment (Kosmatka and Wilson, 2011; Mehta and Monteiro, 2006; Brooks, 2000). Drying shrinkage is similar to autogenous shrinkage in that the internal water pores are affected. However, drying shrinkage only occurs when the system is exposed to an external drying

environment. If the system is sealed, as is the case in oil well construction, drying shrinkage will likely be irrelevant. For this reason, drying shrinkage was not considered as part of this shrinkage study.

2.5.4 Shrinkage Mitigation Techniques

Zonal isolation, or the prevention of the flow of liquid and gases in an oil well cementing site, is critical to the well's structural integrity and hydraulic annular or plug seal. If zonal isolation is lost due to the inherent dimensional changes of the cementing material, this causes a serious environmental issue requiring timely and expensive repair operations. To combat this issue, industry professionals have turned to alternative materials with lesser dimensional changes under downhole temperature and pressure conditions. Such materials include bismuth and thermite or other swelling polymers. Though these materials work, in theory, the use of such alternatives comes at much higher cost than OPC slurries, and these materials are challenging to place in the well (Soucy et al., 2017).

Shrinkage-compensating cements have been studied as early as the 1920s and are available and designated as Type E-1, according to ASTM C845 (2018), but these cements are unsuitable as oil well cement slurries. Shrinkage-compensating cements are meant to cure under moist conditions and preferably in reinforced and/or post-tensioned concrete applications, which is not the case in oil well cementing (Carter, 1966). Alternatively, the use of aluminum as a gas generating admixture for shrinkage control was employed originally in structural concrete applications, but later tested by Carter (1966) for oil well applications. Carter's (1966) work focused on adding finely powdered aluminum to react with the alkalis in the cement slurry, which would produce hydrogen bubbles, which would then aid in expanding the cement slurry. The method of aluminum addition has continued to be studied and has been proven as a successful method of shrinkage control. However,

there are significant issues with its use in high pressure high temperature (HPHT) conditions, as is the case in oil wells (Carter, 1966; Soucy et al., 2017). Specifically, at these HPHT conditions the expansive reaction is over in as early as 30 minutes because of the elevated temperature, and the bubbles created may be too small due to the elevated pressure (Carter, 1965; Soucy et al., 2017). Beyond the issues at HPHT, there are also safety concerns with handling and mixing using this method regarding ventilation and storage.

As a continuation of the work on aluminum additives for shrinkage control, a novel method of aluminum, as well as zinc, addition has been developed and was evaluated in this work on both OPC and geopolymers. These expansive agents allow for stable storage, improved handling, and can either accelerate or retard the expansion allowing for use in oil well cementing operations. Further discussion on how this was accomplished is presented in Chapter 3.

CHAPTER 3 : MATERIALS AND METHODS

This chapter provides a description of the various materials and experimental protocols used to evaluate OPC and geopolymer shrinkage. Section 3.1 contains information about the raw materials used to prepare both OPC and geopolymer slurries. Section 3.2 describes the standardized laboratory testing techniques used to evaluate shrinkage, along with a novel shrinkage measurement method developed during this study.

3.1 RAW MATERIALS

3.1.1 Cementitious Materials

The oxide compositions of the fly ash and OPC used during this study are presented in Table 3.1. The oxide composition of the OPC was obtained from the mill certificate provided by the manufacturer while the fly ash oxide composition was determined using an x-ray fluorescence technique procedure as prescribed in ASTM C311-13 (2013). The chemical composition of the fly ash used for this study is representative of Class F fly ash in accordance with ASTM C618-17 (2017). This type of fly ash was selected for analysis based on its low calcium content (~3% CaO) and similarity in composition to fly ash in previous, successful oil well geopolymer mixtures (Liu 2017; Liu et al., 2016). The oxide composition and particle size distribution of the OPC used in this study were representative of a Class H OPC, which is typically used for oil well cementing operations. OPC slurries were prepared by mixing Class H OPC with water (0.385 water to cement ratio by weight) following the procedure described in API RP 10B-2 (2010).

Note: Portions of this chapter content were previously published in Olvera, R., Panchmatia, P., Juenger, M., Aldin, M., and van Oort, E., 2019. Long-term Zonal Isolation Control Using Geopolymers: An Analysis of Shrinkage Behavior. Published in SPE/IADC International Drilling Conference and Exhibition. The author of this thesis was the main author who wrote the paper while the co-authors provided editing and technical verification.

Table 3.1: Oxide composition of Class F fly ash and Class H OPC employed in this study.

Component	Weight %	Weight %
	Class F fly ash	Class H OPC
SiO ₂	46.45	22.1
Al ₂ O ₃	24.09	2.7
Fe ₂ O ₃	20.05	4.5
(SiO ₂ +Al ₂ O ₃ +Fe ₂ O ₃)	90.59	29.3
CaO	3.08	64.4
MgO	0.79	2.5
Alkalis (Na ₂ O+0.658K ₂ O)	1.88	0.2
SO ₃	0.52	2.8
TiO ₂	1.15	N.A.
LOI (750°C)	0.82	1.1

3.1.2 Activator Solution and Geopolymer Preparation

The activator used in this study was an 8M sodium hydroxide solution. This activator solution was selected because it resulted in a geopolymer with rheological and mechanical properties that was shown to be suitable for oil well cementing applications (Liu, 2017; Liu et al., 2016). In addition, others have reported in the literature that 8M NaOH solution successfully activated geopolymers (Aughenbaugh, 2013; Duxon et al., 2006; Provis and Deventer, 2009).

The 8M NaOH solution was prepared using commercially-available NaOH pellets (99% purity), which were dissolved in appropriate amounts of deionized water (resistivity of 18 MΩ) using a magnetic stirrer. Fly ash was mixed with the 8M NaOH solution to create the geopolymer slurry. The NaOH to fly ash ratio was maintained at 0.485 by weight for optimum strength and workability (Liu, 2017; Liu et al., 2016). Geopolymer slurries were initially hand-mixed to obtain a uniformly blended mixture and then mixed with an overhead paddle stirrer which was operated at 480 rpm for 30 seconds.

It is important to note that sodium hydroxide solutions experience a significant temperature increase during preparation due to their high enthalpy of dissolution. In addition, the hydroxide activator also has a high pH. Thus, caution must be taken when handling the hydroxide solution. Once the geopolymer hardens, the hydroxide and the alkali ions are chemically bound and therefore pose little or no threat to the surrounding environment. Thus, the final product is safe to use for any application for which it is suitable.

3.1.3 Synthetic-Base Mud (SBM)

NAFs have low friction coefficients and are frequently used in oil well cementing to aid in shale stabilization and fluid loss control; but, despite the use of spacer fluids, NAFs often remain and contaminate OPC slurries. Even at low contamination levels (5%), NAF significantly affects the strength and rheological properties of an OPC slurry, reducing the probability of zonal isolation. In contrast, fly ash-based geopolymers have shown good mechanical and rheological properties when contaminated by NAF (Liu, 2017). However, there has been no evaluation of the effects of contamination on the shrinkage behavior of both OPC and geopolymer slurries. Therefore, it warrants study into how NAF contamination affects shrinkage behavior in both OPC and geopolymers.

To study the effects of NAFs, SBM was added into the OPC and geopolymers formulated in this study. The properties of SBM used in this study are shown in Table 3.2. SBM was added into OPC and geopolymer mixtures to simulate contamination in the oil well, but also as a means to prove that SBM can be solidified by the geopolymer. Geopolymer-hybrids were prepared by mixing (10% or 20% volume replacement of SBM into the already prepared geopolymer slurry using an overhead paddle stirrer operated at

480 rpm. Similarly, SBM was mixed into OPC slurries to obtain OPC-SBM hybrids with 10% and 20% (by volume) SBM.

Table 3.2: Properties of the SBM formulation used in this study.

Density (ppg)	9.63
CaCl ₂	19.19%
synthetic/water ratio (SWR)	76.4/23.6
Water	20.5%
Oil	66.5%
Solid	13%

3.1.4 Expansive Agents

Expansive agents were added into geopolymer and OPC slurries to evaluate their ability to reduce shrinkage. Specifically, zinc- and aluminum-based expansive agents were used in this study. Table 3.3 and Table 3.4 show the approximate composition of these additives. These expansive agents work by generating hydrogen bubbles when reacting in the geopolymer or OPC slurry. The point of the hydrogen gas creation was to counteract volume reduction tendencies by creating space and spreading out the slurry, though not to the point where porosity becomes an issue. The zinc- and aluminum-based expansive agents were mixed into the activating solution or the water used to create the geopolymer slurry or the OPC slurry, respectively. The dosages of zinc-based expansive agent used in this study were 0.05% and 0.09% (by weight of cement/fly ash). For the aluminum-based expansive agent, the dosages were set at 0.2% and 0.4% (by weight of cement/fly ash). These values were arrived at by a trial and error method by observing the stability of mixtures with different dosages of expansive agent during initial testing of mixtures at room temperature.

As stated in Chapter 2, there are safety concerns associated with the use of metal-based expansive agents. When used as fine powders, these expansive agents are inherently dusty (producing respiratory concerns) and can be explosive if not properly handled. To combat this problem, the expansive agents used in this study were combined (by the supplier) with other base oils and mutual solvents to form a safe and stable slurry. By forming a slurry, the base oils work similar to encapsulators, which can then be used to control the timing and rate of hydrogen gas generation (Soucy et al., 2017).

Table 3.3: Composition of zinc-based expansive agent.

Zinc	~25%
Glycol	~75%

Table 3.4: Composition of aluminum-based expansive agent.

Aluminum	~25%
Glycol	~75%

3.2 EXPERIMENTAL METHODS

Though AAM work is still in its early stages, there does exist published literature regarding volumetric changes in geopolymers and AAM. However, much of this published literature contains contrasting results and theories (Provis and van Deventer, 2014). From a thermodynamic theory consideration, AAM mixtures should be more prone to volume reductions than OPC because the final reaction products have a greater gel porosity than that of the final hydration products found in OPC slurries (Chen and Brouwers, 2007; Thomas and Jennings, 2012). However, upon actual testing on mortar and concrete specimens, results have shown that AAM experience less shrinkage than OPC-based systems (Provis and van Deventer, 2014). Unlike OPC mixtures whose chemical reactions have been meticulously studied for centuries, our understanding of geopolymer reaction

mechanisms is still primitive. When testing for autogenous shrinkage, for example, published literature explains that while autogenous shrinkage is still measurable in geopolymers, the resulting autogenous shrinkage measurement are due to the continuous reorganization and polymerization of the geopolymer, rather than the self-desiccation process present in OPC mixtures (Ma and Ye, 2014). For alkali-activated fly ash materials, performance and properties vary due to a number of factors including curing method, excess water availability, early age drying conditions, and general mix design. Furthermore, the type of activator, activator concentration, aluminosilicate type, and the mixture proportions between the precursor powder and the activator also affect behavior (Neto et al., 2008; Yusuf et al., 2014; Atis et al., 2017; Bakharev et al., 1999).

Another issue with the measurement of shrinkage is the current testing protocols. As previously mentioned, OPC shrinkage theory and mechanisms have been used in literature to evaluate geopolymer shrinkage behavior, though some testing methods may not be suitable for testing geopolymers (Provis and van Deventer, 2014). In OPC testing, for example, lime-water is used to provide a Ca^{2+} rich environment to prevent decalcification in OPC binders. Using lime-water in geopolymers, however, will actually promote alkali loss, especially when the AAM system is immersed in a calcium-rich solution at early ages (Provis and van Deventer, 2014).

The two primary shrinkage mechanisms tested in this study were autogenous and chemical shrinkage. Specifically, the capillary tube test was performed in accordance to ASTM C1608-17 (2017) to test for chemical shrinkage, while the membrane test was carried out according to API 10B-5 / ISO 14026-5 (2010) to evaluate autogenous shrinkage. Both of these testing methods were performed at 23°C and 50°C. Testing at 80°C was carried out as well, in an effort to simulate the higher oil well temperatures; but testing at such temperatures resulted in erroneous data due to the limitations of the set-up

prescribed in the standardized tests. A further discussion of this issue is presented in the capillary tube and membrane test sections of Chapter 3.2. All experiments were performed at atmospheric pressure using these testing methods.

With both testing methods, at least two replicates were tested for each mixture design in order to confirm results and repeatability. Following the recommendation from ASTM C1608-17 (2017), data acquisition started an hour after mixing for both the capillary tube and membrane test. This waiting period allowed for all samples to reach thermal equilibrium at the designated testing temperature, eliminating any temperature differential artefacts. Preliminary testing demonstrated that the majority of sample shrinkage occurred during the first 48 hours of hydration or polymerization and the rate of shrinkage plateaued after 120 hours. Therefore, data were collected for only 120 hours (5 days).

3.2.1 Capillary Tube Test

The capillary tube test was performed as prescribed in ASTM C1608-18 to measure the chemical shrinkage in both OPC and geopolymer slurries. Figure 3.1 shows the setup employed in this study. Slurry samples were placed into a plastic vial to a height of 5-10 mm and filled with de-aired water. A capillary tube (fixed and sealed inside a rubber stopper) was then inserted into the vial tight enough to remove entrapped air. Insertion of the tube into the vial created a rise in water into the capillary. Paraffin oil was then poured at the top of the water level to prevent evaporation of water (especially at the higher temperatures). Finally, the vial was then submerged in a water bath (or oil bath for elevated temperatures) maintained at the designated testing temperature to achieve isothermal conditions. Measurements of the water level in the capillary tube were recorded every hour (or more often) for the first 8 hours, and then periodically for the remaining 120 hours.

These water level measurements were converted to shrinkage values (expressed in ml/g of sample) using the following equation:

$$V_{cs} = \frac{H_x - H_0}{M_{paste}}$$

Where:

V_{cs}	= volume at a particular time	[ml/g of sample]
H_x	= water level at the time of interest	[ml]
H_0	= water level 60 minutes after mixing	[ml]
M_{paste}	= mass of the sample	[g of sample]

It should be noted that capillary tube testing was also performed at 80°C, but the replicates showed significant variability likely due to the evaporation of water within the tube. Thus, the results for 80°C using the capillary tube test are not presented in this thesis. The max level of error was ± 0.006 ml/g of sample. For samples not showing any error bars, the error was so low that error bars were omitted.



Figure 3.1: Capillary tube test setup employed in this study.

3.2.2 Membrane Test

The membrane test utilizes the standardized test method listed in API 10B-5 / ISO 14026-5 (2010) to quantify autogenous shrinkage. In this test, a slurry sample is placed and sealed in a flexible, impermeable membrane. For proper data collection, sufficient agitation of the sample is needed to eliminate air bubbles before sealing the slurry into the impermeable membrane. Next, the sample was suspended from a balance while being fully immersed in an oil bath maintained at the designated testing temperature. As hydration/polymerization progresses, there is a corresponding change in overall sample volume, which was indirectly measured by the change in the buoyancy of the suspended

sample. These buoyant weight measurements were then used to calculate the percent bulk volume change according to the following formula:

$$V_{as} = \frac{V_f - V_i}{\rho * V_i} * 100$$

Where:

- V_{as} = percent volume at a particular time [%]
 V_f = $M_a - M_{fm}$ = final volume of the slurry [ml]
 V_i = $M_a - M_{im}$ = initial volume of the slurry [ml]
 ρ = density of oil [g/ml]

Where:

- M_a = mass in air of the slurry [g]
 M_{im} = initial measured mass of the submerged slurry [g]
 M_{fm} = measured mass of submerged slurry at time of interest [g]

Note: The max level of error was ± 0.31 the reported value.



Figure 3.2: Membrane test setup used in this study.

3.2.3 Isothermal Calorimetry

With chemical shrinkage occurring as a result of cement hydration, isothermal calorimetry could complement chemical shrinkage results by correlating the heat released from samples to the chemical shrinkage. Past studies on shrinkage have shown that the total chemical shrinkage is proportional to cumulative heat evolution if tested at the same temperature (Pang et al., 2013). Isothermal calorimetry was thus performed on OPC and geopolymer slurries in accordance with ASTM C1679 (2017) to measure the heat evolution during hydration/polymerization reaction. In this test, 9-10 grams of OPC or geopolymer

slurry was sealed in a glass ampule and lowered into a Tam Air Isothermal Calorimeter (Thermometric) which was maintained at the designated temperature. At the same time, an ampoule filled with an appropriate amount of water such that the heat capacity of the water was equal to that of the cement/geopolymer sample was lowered into the reference cell. Once in the calorimeter, the difference in outputs between the sample heat flow sensor and the reference heat flow sensor could be measured to determine the heat released from hydration in the OPC slurry or polymerization in the geopolymer. The resulting power outputs from the calorimeter were analyzed to get the cumulative heat of hydration/polymerization of the slurries. At least three replicates were tested for each mixture design in order to confirm results and repeatability. Note: the maximum level of error was ± 2.46 mW/g the reported value for cumulative heat released data.

3.2.4 Diaphragm Accumulator Test

The principles behind shrinkage measurements and data collection in the capillary tube and membrane tests are fairly simple, and the ASTM and API standards carefully regulate measurements for consistency and accuracy. Nevertheless, there are issues with each test that may be complicating data collection. For the capillary tube test, for example, it is difficult regulate the amount of water going into the tube as well as the amount of sample in each vial. Therefore, sample thickness and surface water on the sample may be inconsistent. Previous research on the effect of these variables on the measured chemical shrinkage has shown that greater amounts of water in the capillary tube promotes a higher rate of chemical shrinkage before the induction period and reduces the amount of chemical shrinkage that occurs during later stages of hydration due to dilution and Ca^{2+} leaching out of the paste into the water (Sant et al., 2006). In addition, increased sample thickness was found to result in reduced chemical shrinkage due to either reduced permeability or dilution

in thin samples (Sant et al., 2006; Geiker, 1983). When testing at higher temperatures, as is the case in this study, evaporation of water from the capillary tube also presents an issue. In order to reduce evaporation effects, a larger paraffin oil barrier can be used, but it may not fully prevent evaporation as observed by the inconsistencies in results obtained from tests conducted on the same slurry at 80°C. In the membrane test, temperature is also a limiting factor. Testing at 80°C, and even 50°C, caused the flexible membrane to melt, and resulted in inaccurate data.

Another issue affecting both the capillary tube and membrane test is the inability to test samples under elevated pressures. In each test, the samples are only exposed to ambient pressure. This shortcoming in testing prevents a full understanding of how these slurries may perform under downhole conditions. The lack of pressure during testing also presented an artefact in testing when the use of hydrogen-creating expansive agents were introduced into the mixture. For example, capillary tube results showed some expansive behavior during initial measurement, though at later stages shrinkage at equal magnitudes as the neat OPC and geopolymer was recorded. With the creation of hydrogen bubbles as a shrinkage mitigation approach, it was hypothesized that a portion of the shrinkage measured in the capillary tube was likely due to hydrogen leaving the cement matrix in addition to the shrinkage of slurry. Thus, a new testing method (utilizing a diaphragm accumulator) was developed to evaluate the shrinkage behavior of OPC and geopolymer slurries under downhole conditions and the effectiveness of zinc- and aluminum-based expansive agents in mitigating shrinkage in OPC and geopolymer systems.

A diaphragm accumulator consists of a thick steel shell with a fillable flexible diaphragm on one end and a gas valve on the other end, as shown in Figure 3.3. To perform shrinkage measurements, slurries were poured and sealed into the flexible diaphragm while oil was pumped using hydraulic pumps on the opposite end. The hydraulic pumps (with

0.02% accuracy) allowed for pressure to be maintained at the designated value (which ranged from 200 to 2000 psi). The diaphragm accumulator set-up was placed inside a temperature-controlled oven with horizontal air flow for precise temperature measurements ranging from 35 to 80 °C. Figure 3.4 illustrates the set up employed in this study. As the slurry shrinks/expands, the hydraulic pump inserts or extracts oil into the set-up to maintain the designated pressure. The change in the volume of oil required to maintain pressure in the accumulator is therefore a measure of the change in volume of the slurry in the flexible membrane. The use of this system allowed for accurate measurement of shrinkage when the slurries were tested under high pressure high temperature conditions. Furthermore, this set-up prevented the escape of hydrogen gas produced when expansive agents were added to the slurries and therefore provided an accurate measure of the effects of expansive agents on the shrinkage behavior of OPC and geopolymer slurries.

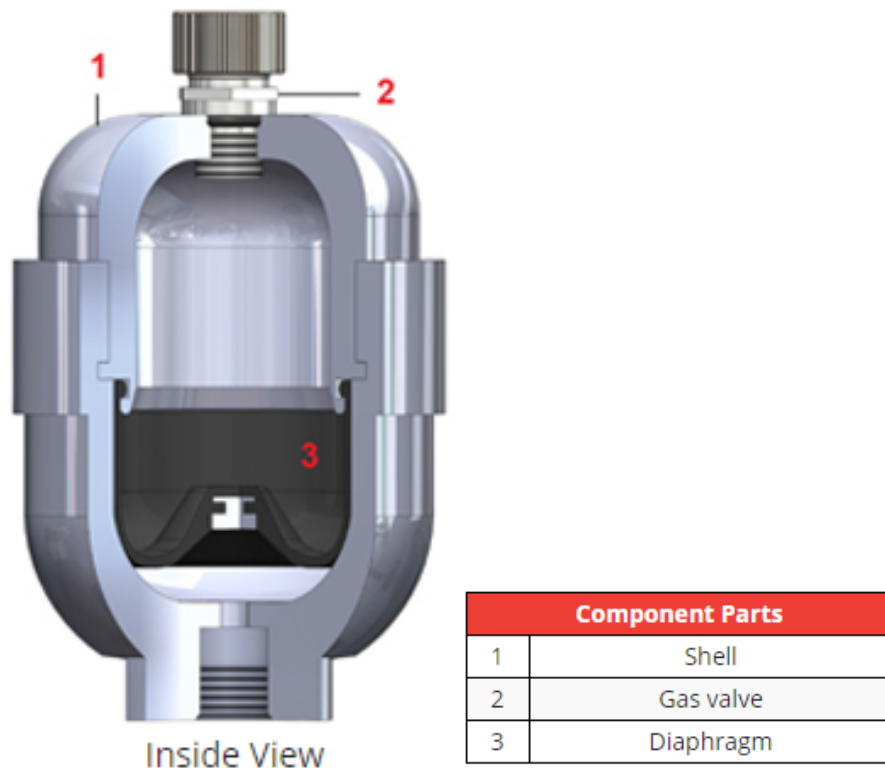


Figure 3.3: Diaphragm accumulator components. Obtained from the Accumulators, Inc. (diaphragm accumulator manufacturer) website (<https://www.accumulators.com>, 2019).



Figure 3.4: Diaphragm accumulator set-up employed in this study.

3.2.5 Optical Microscope Imaging

In order to verify the effects of the zinc- and aluminum-based expansive agents, optical microscope imaging was performed on diaphragm accumulator samples. To prepare samples for microscopic imaging, the diaphragm accumulator samples were sawn off from each end and a cross-section from the middle of the sample was retrieved. Next, the sample was polished using sand paper in the following order of grit size: 120, 400, 600, 800, and 1200 until a smooth polished surface was reached. Between each polishing session, the samples were immersed in an ethanol filled beaker placed in an ultrasonic

cleaner to remove any excess grit from polishing. Once fully polished and cleaned, an optical microscope was used to photograph samples microscopically at 0.8x magnification. Figure 3.5 present a sample after polishing. It should be noted that polishing of geopolymer was attempted, but samples were not solid enough to be properly smoothed. Thus, only OPC samples will be discussed in Chapter 4.

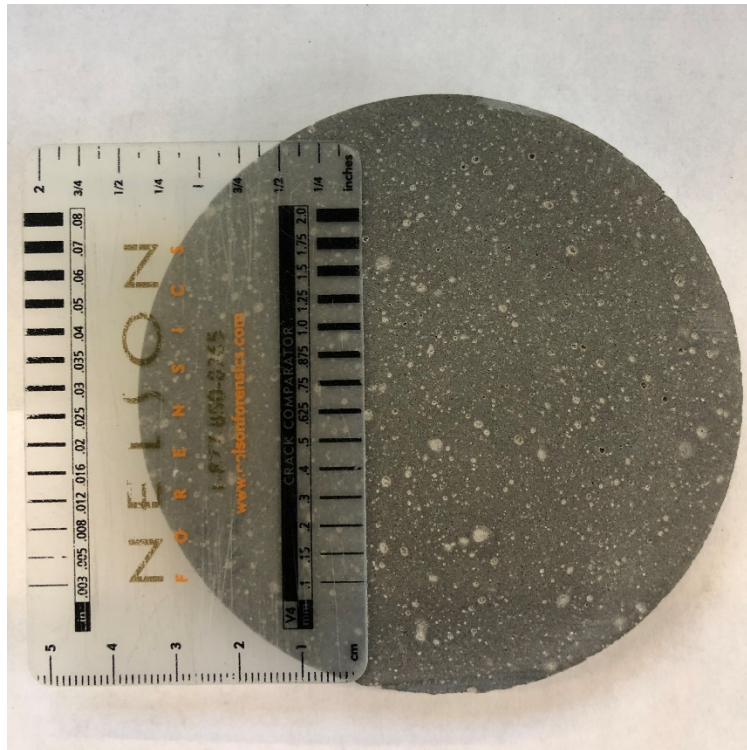


Figure 3.5: Diaphragm accumulator sample after polishing.

CHAPTER 4 : RESULTS AND DISCUSSION

This chapter contains the results obtained from standardized and unconventional shrinkage testing conducted during this study. Specifically, results characterize the shrinkage behavior of OPC and geopolymer slurries subjected to different curing temperatures, SBM contamination levels, expansive agents, and pressure conditioning. These results were used to evaluate the potential of fly ash-based geopolymers to be used for oil well cementing applications. Isothermal calorimetry and optical microscopy were also conducted to supplement and/or explain the observations made during shrinkage testing. Results from those tests are also presented in this chapter.

4.1 OPC AND GEOPOLYMER SHRINKAGE BEHAVIOR

The effects of temperature on the chemical and autogenous shrinkage behavior of OPC and geopolymer slurries were examined using the capillary tube and membrane test, respectively. Figure 4.1 presents the chemical shrinkage (measured by the capillary tube tests) experienced by both OPC and geopolymer (labeled as FA) slurries when tested at 23°C and 50°C. Note: The max level of error was ± 0.006 ml/g of sample of the reported number using the capillary tube test. At room temperature ($T = 23^{\circ}\text{C}$), the OPC slurry shrank 0.022 ml/g of sample after the 120-hour testing period. Meanwhile, the geopolymer slurry shrank considerably less than the OPC slurry when tested at 23°C (i.e. 0.009 ml/g of sample after 120 hours). With an increase in temperature from 23°C to 50°C, both OPC and geopolymer slurries experienced an increase in total chemical shrinkage. However, at

Note: Portions of this chapter content were previously published in Olvera, R., Panchmatia, P., Juenger, M., Aldin, M., and van Oort, E., 2019. Long-term Zonal Isolation Control Using Geopolymers: An Analysis of Shrinkage Behavior. Published in SPE/IADC International Drilling Conference and Exhibition. The author of this thesis was the main author who wrote the paper while the co-authors provided editing and technical verification.

50°C, the geopolymer slurry experienced a higher magnitude of chemical shrinkage (0.043 ml/g) than OPC slurry (0.031 ml/g) after 120 hours of hydration/polymerization. In addition, it was observed that the rate of shrinkage in the geopolymer slurry was greater than that of the OPC slurry at the end of the testing period (120 hours). This implies that the geopolymer slurry will shrink more as polymerization proceeds. Long-term testing needs to be performed to quantify the total extent of shrinkage for geopolymers cured at 50°C. Capillary tube testing was also performed at 80°C but resulted in unreliable data potentially due to evaporation of water from the capillary tube at such a high temperature. This is one of the limitations of the standardized ASTM C1608-17 (2017) testing method.

The geopolymer and OPC slurry shrank approximately 5 times and 1.5 times more (at 120 hours) when the curing temperature was increased from 23°C to 50°C, respectively. This result suggests that temperature plays a significant role in the shrinkage behavior of both OPC and geopolymer slurries; however, the significance of temperature is much higher for geopolymer slurries. Literature confirms that curing temperature plays a stronger role in the geopolymer polymerization process than the NaOH concentration or liquid-to-solid ratio (Sun and Vollpracht, 2018). Curing at room temperature is possible, but results in low reactivity and requires longer than desirable time to develop measurable strength (Sun and Vollpracht, 2018). The literature also confirms, that a curing regime between 40°C and 100°C, will accelerate the polymerization process and aid in geopolymer strength development (Davidovits, 1989; Duxson et al., 2007; Somna et al., 2011). Research by Singh and Subramaniam (2019) indicates that this may be due to higher reactivity of fly ash at elevated temperatures. When temperature is increased, there are greater amounts of percolated early hydration products because the temperature greatly increases the rate of dissolution of glassy phases in the fly ash (Singh and Subramaniam, 2019). Therefore, the total amount and rate of chemical shrinkage experienced by geopolymers is expected to

increase with temperature because there is a greater densification of the microstructure from increased polymerization. Additional testing to confirm increased rate of polymerization experienced by geopolymers at elevated temperatures is presented in section 4.5.1 of this chapter.

The results from the membrane test, which measures autogenous shrinkage, for both OPC and geopolymer slurries are shown in Figure 4.2. The OPC slurries shrank 4.51% (by volume) whereas the geopolymer slurries shrank only 0.92% (by volume) after 120 hours of hydration/polymerization at 23°C. Note: The max level of error in the membrane test was ± 0.31 the reported value. The results from the membrane test and capillary tube test produced similar trends for both OPC and geopolymers when tested at 23°C. Testing at higher temperatures was not possible because of instability (i.e. melting) of the flexible membrane.

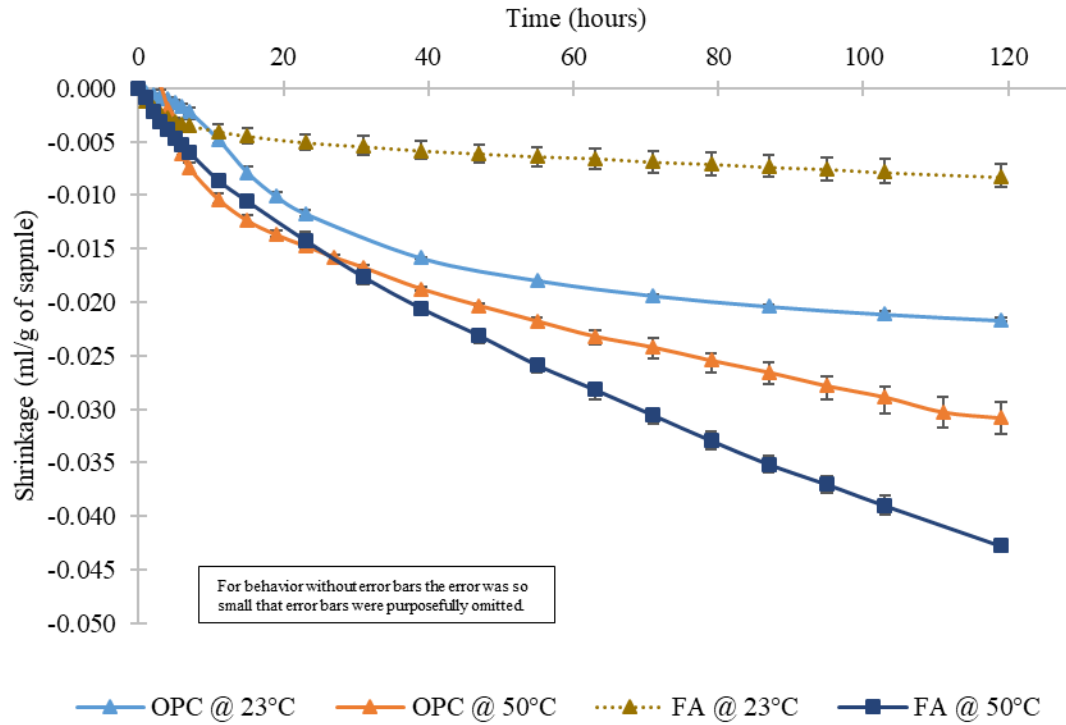


Figure 4.1: Chemical shrinkage in OPC and geopolymer slurries at 23°C and 50°C, measured using the capillary tube test.

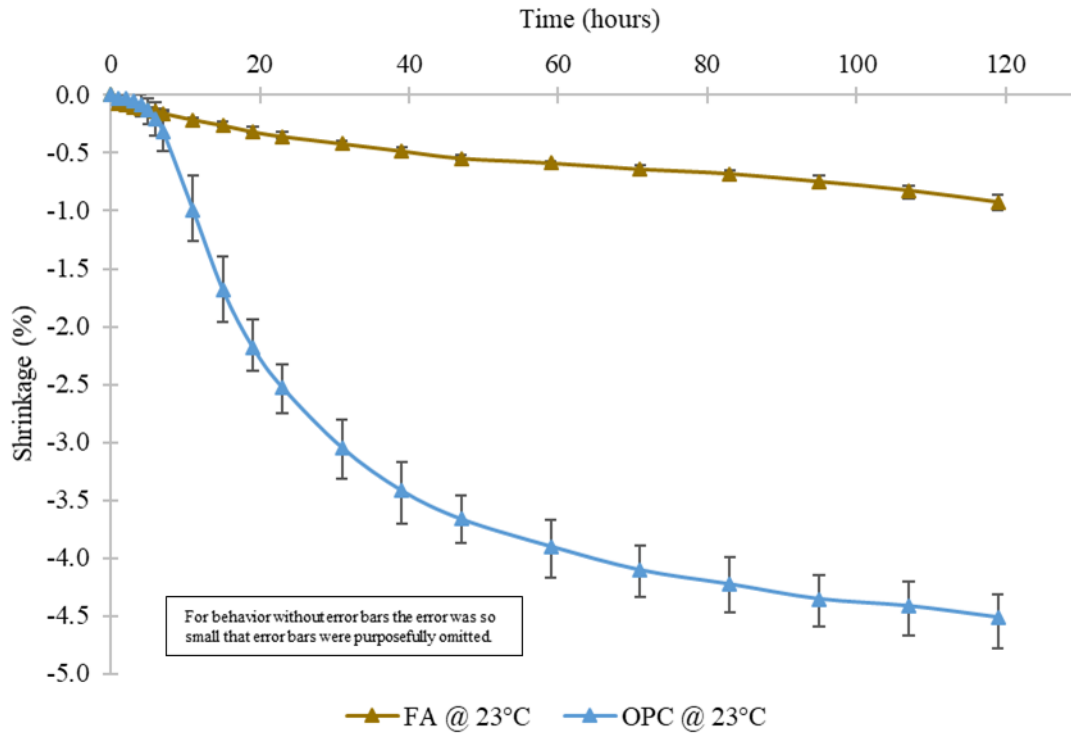


Figure 4.2: Autogenous shrinkage of neat OPC and geopolymer slurries at 23°C, measured using the membrane test.

4.2 EFFECTS OF SBM CONTAMINATION ON THE SHRINKAGE OF OPC AND GEOPOLYMER SLURRIES

Figure 4.3 shows the chemical shrinkage of geopolymer slurries contaminated with 10% and 20% SBM (by volume). The addition of SBM resulted in an increase in chemical shrinkage of geopolymer slurries tested at both 23°C and 50°C. At 23°C, the addition of both 10% and 20% SBM (by volume) in geopolymer slurries increased the chemical shrinkage of the slurry from 0.009 ml/g to 0.021 ml/g after 120 hours. At 50°C, SBM contamination of 10% and 20% (by volume) resulted in an increase in chemical shrinkage from 0.043 ml/g to 0.048 ml/g and 0.074 ml/g, respectively, at 120 hours. It should be noted that increasing the SBM contamination from 10% to 20% had little effect on the chemical shrinkage of geopolymers tested at 23°C. However, for geopolymer slurries

tested at 50°C, 10% and 20% SBM contamination levels showed significant differences (72% increase) in the recorded chemical shrinkage. Additionally, adding 10% SBM into the geopolymer slurry did not significantly increase its chemical shrinkage (only 12% increase) when tested at 50°C.

Figure 4.4 shows the chemical shrinkage of OPC slurries contaminated by SBM. At 23°C, contamination of OPC slurries with 10% and 20% SBM (by volume) resulted in an increase in chemical shrinkage from 0.022 ml/g to 0.037 ml/g and 0.046 ml/g at 120 hours, respectively. The addition of 10% and 20% SBM into OPC slurries at 50°C resulted in an increase in chemical shrinkage from 0.031 ml/g to 0.052 ml/g of sample and 0.064 ml/g at 120 hours, respectively.

Overall, it was found that the magnitude of chemical shrinkage experienced by OPC slurries (with or without SBM contamination) was greater than that experienced by geopolymers (with or without SBM contamination) when cured at room temperature (23°C). When cured at elevated temperatures (i.e. 50°C), geopolymer slurries experienced higher chemical shrinkage than OPC slurries when they contained 20% SBM (by volume). On the other hand, geopolymer slurries with 10% SBM contamination showed slightly lower chemical shrinkage than OPC slurries contaminated with 10% SBM (by volume). Furthermore, Figure 4.3 also confirms that temperature has a significant effect on geopolymer shrinkage.

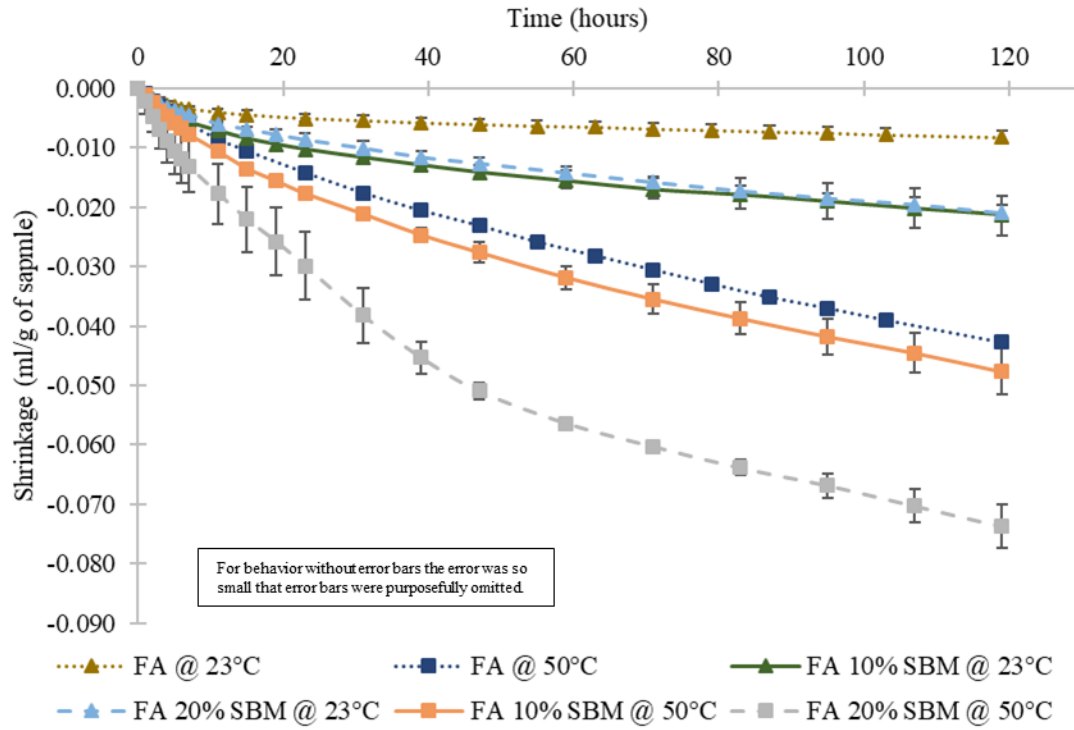


Figure 4.3: Chemical shrinkage of geopolymer slurries contaminated with SBM, measured using the capillary tube test.

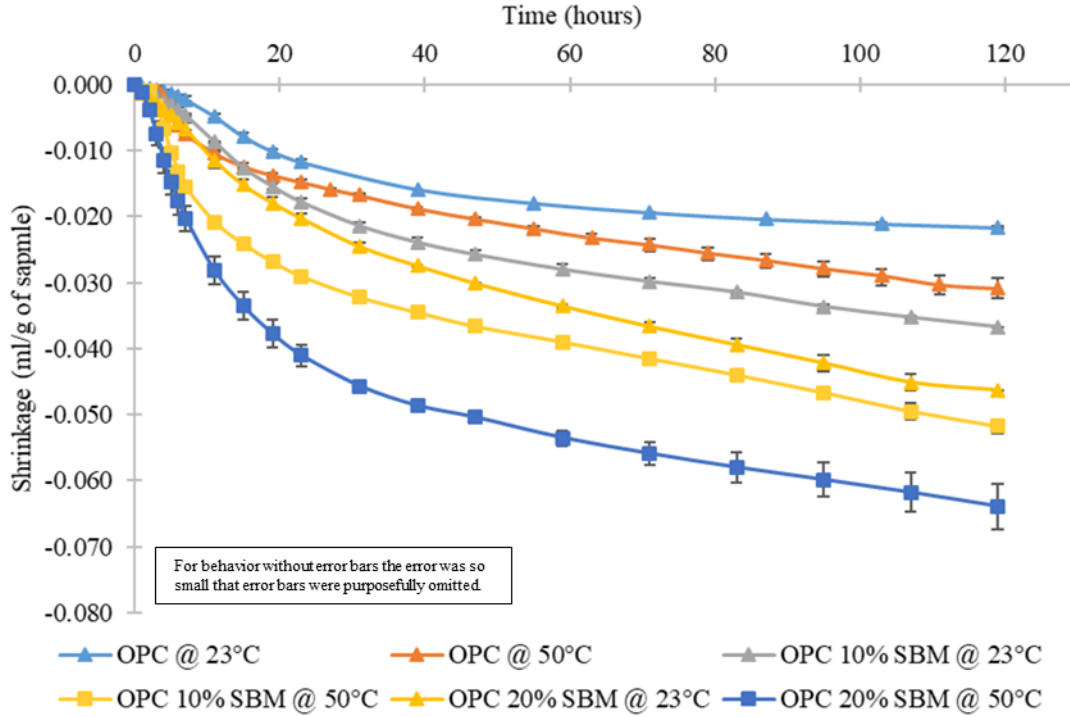


Figure 4.4: Chemical shrinkage of OPC slurries contaminated with SBM, measured using the capillary tube test.

4.3 HEAT OF HYDRATION COMPARISON TO SHRINKAGE

Previous studies have confirmed that the cumulative heat of hydration of OPC slurries is proportional to its chemical shrinkage (Pang et al., 2013). Thus, isothermal calorimetry was performed on geopolymer slurries to verify if the same theory can be applied to the polymerization process in alkali-activated materials. Isothermal calorimetry results for both geopolymer and OPC slurries performed at 23°C and 50°C are shown in Figure 4.5 and Figure 4.6, respectively. Cumulative heat results for slurries tested at 23°C and 50°C are presented in Figure 4.7 and Figure 4.8, respectively. Note: the maximum level of error in the isothermal calorimetry results for cumulative heat released was ± 2.46

mW/g the reported value. Compared to the magnitude of results this error was small. Thus, error bars were purposefully omitted.

At 23°C, the rate of heat release curve for OPC slurries had only one distinct peak. At this temperature, OPC slurry released an average of 58.25 mW/g of sample of heat after hydrating for 120 hours. After 120 hours of hydration, the slope of the cumulative heat of hydration curve for OPC was small (0.1 mW/g-hr). This means that the majority of the hydration had occurred by 120 hours, and we can thus conclude that the chemical shrinkage experience by the slurry after this point will be negligible (relative to the total chemical shrinkage experienced up to 120 hours of hydration). Comparing the plot for the cumulative heat of hydration for OPC at 23°C (as shown in Figure 4.7) to that of chemical shrinkage of OPC at the same temperature (Figure 4.1) shows that there is a proportional relationship between chemical shrinkage and cumulative heat of hydration for OPC slurries. Both plots plateau in similar fashion around the same hydration time. A similar trend between chemical shrinkage and the cumulative heat of hydration was observed for geopolymer slurries tested at 23°C.

For geopolymers tested at 23°C, the rate of heat release is almost flat (Figure 4.5), and there is very minimal heat released after 120 hours (only 7.60 mW/g). Comparing the geopolymer calorimetry results at 23°C from Figure 4.7 to the chemical shrinkage results from Figure 4.1, it is again clear that the two trends are similar, indicating that the degree of polymerization occurring in geopolymer slurries is proportional to the chemical shrinkage experienced by those slurries. With an increase in temperature from 23°C to 50°C, the cumulative heat released increased from 58.25 mW/g to 67.18 mW/g (a 15.33% increase) for the OPC slurry after completing 120 hours of hydration (as shown in Figure 4.8). Similar to the observation made for OPC slurries tested at 23°C, the heat of hydration for OPC slurry tested at 50°C had a single peak (with a magnitude of 8.62 mW/g of

sample), as shown in Figure 4.7. For geopolymer slurries, increasing the temperature from 23°C to 50°C resulted in an increase of 277% (from 7.60 mW/g to 28.66 mW/g) in the total heat released after undergoing 120 hours of polymerization reaction. It is important to note that the total heat released during polymerization of geopolymer at 50°C was 42.7% lower than that released during the hydration of the OPC at the same temperature. Yet, geopolymer slurries experienced 38.7% more chemical shrinkage than OPC slurries when tested at 50°C. Therefore, there is no direct correlation between heat of hydration/polymerization to the magnitude of chemical shrinkage experienced by the different cementitious materials because the enthalpies of the chemical reactions are different for hydration and polymerization. Similar to the OPC slurry, however, the amount of heat released by geopolymer slurries appears to be proportional to the magnitude of the chemical shrinkage experienced by the material. For geopolymer slurries, the ratio of the shrinkage recorded after 120 hours when tested at 23°C and 50°C was 0.21:1 whereas the ratio of cumulative heat released at 23°C and 50°C after 120 hours was 0.26:1. It should also be noted that at 50°C, the geopolymer had two distinct peaks in its rate of heat release curve, seen in Figure 4.6. Further discussion on this topic will be presented in section 4.5.1 of this thesis.

It should also be noted that for geopolymers there is a distinct inflection point in the cumulative heat released occurring after 6 hours when set at 50°C, but no such point exists in the heat curve at 23°C. This inflection point was not present in neither the 23°C or 50°C chemical shrinkage results using the capillary tube. Additional discussion on this item will be presented in section 4.5.1 of this thesis.

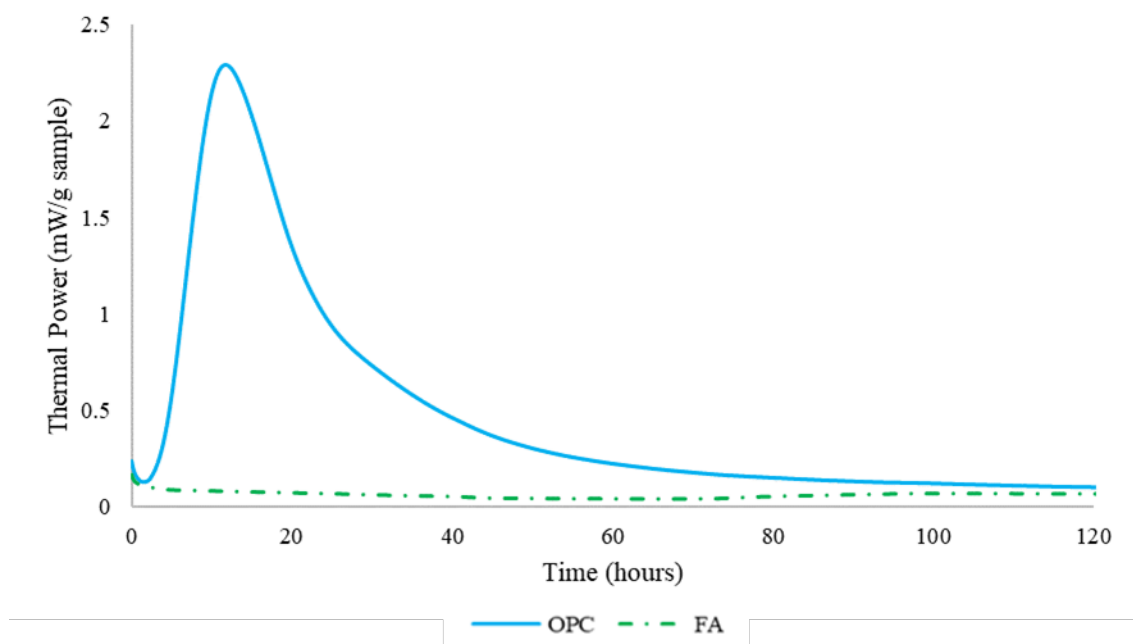


Figure 4.5: Rate of heat release at 23°C, as measured by isothermal calorimetry.

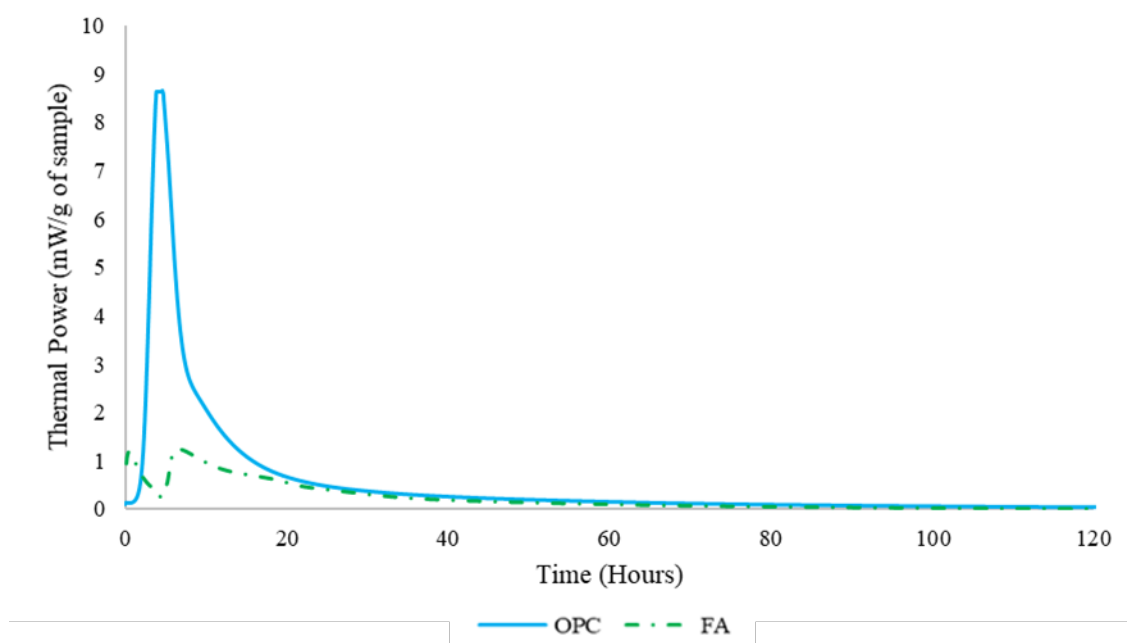


Figure 4.6: Rate of heat release at 50°C, as measured by isothermal calorimetry.

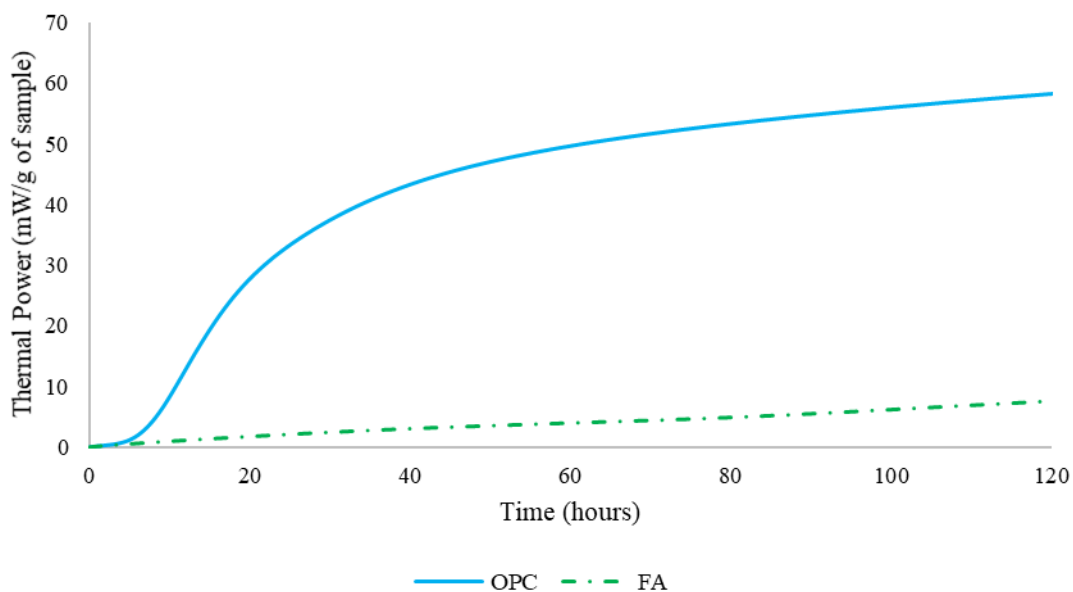


Figure 4.7: Cumulative heat released by OPC and geopolymers at 23°C, measured using isothermal calorimetry.

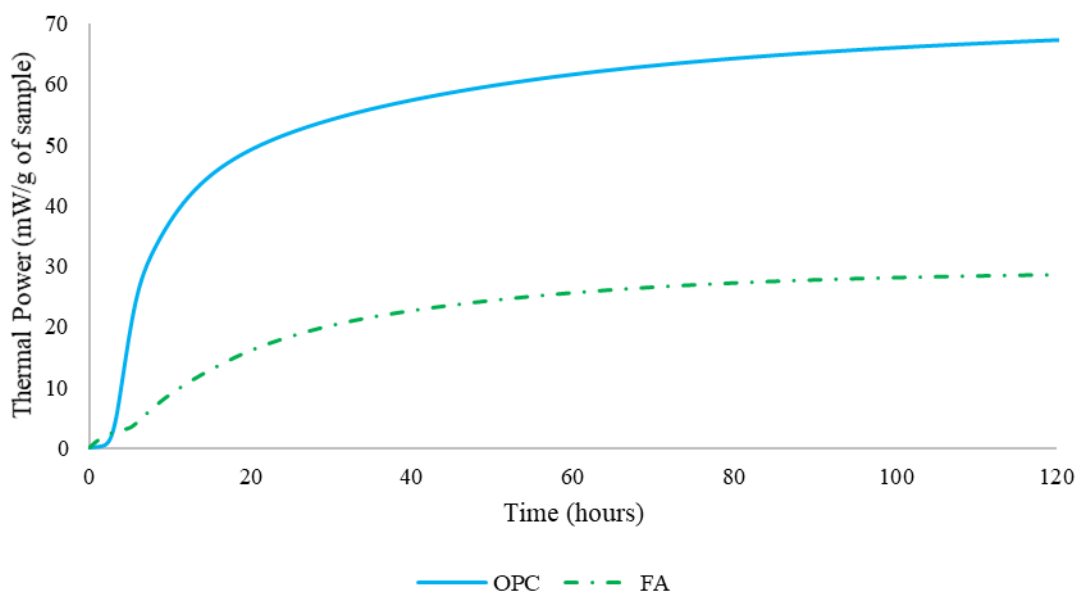


Figure 4.8: Cumulative heat released from OPC and geopolymer mixes at 50°C, measured using isothermal calorimetry.

4.4 EFFECT OF EXPANSIVE AGENTS ON OPC AND GEOPOLYMER SHRINKAGE BEHAVIOR

As seen in the previous sections of this chapter, significant shrinkage occurs in both OPC and geopolymer slurries, especially at elevated temperatures with or without SBM contamination. Therefore, it is essential to develop a viable solution to mitigate and/or counteract the shrinkage in these slurries to make them better suited for oil well cementing. Zinc- and aluminum-based expansive agents were added to both OPC and geopolymer slurries to mitigate their shrinkage. Figure 4.9 and Figure 4.10 present the shrinkage behavior for geopolymers slurries with zinc- and aluminum-based expansive agents, respectively, tested at 23°C and 50°C using capillary tube testing. For slurries tested at 50°C, the inclusion of zinc- or aluminum-based expansive agents provided no indication of shrinkage reduction as all combinations tested resulted in chemical shrinkage similar to those observed for geopolymer slurries without expansive agents. Furthermore, the addition of aluminum-based expansive agent to geopolymer slurries resulted in greater shrinkage than that recorded for plain geopolymer slurries at 23°C. On the other hand, the addition of zinc- based expansive agent showed volume increase (instead of shrinkage) during the first 10 hours of testing at 23°C. However, the final shrinkage for this slurry was still greater than that of the geopolymer without expansive agent.

As shown in Figure 4.11, the patterns for chemical shrinkage observed for OPC slurries containing zinc- and aluminum-based expansive agents had some similarity to those observed for geopolymers with expansive agents. Over the duration of the 120-hour testing period, OPC slurries with zinc-based expansive agents shrank similarly or more compared to OPC slurries without expansive agents when tested at both 23°C and 50°C, despite some expansive behavior observed during the early stages of hydration. With the aluminum-based expansive agent at 23°C and a dosage of (0.2% by weight of fly ash) there was a net positive volume change for about 40 hours before the expansive effects were

overcome by shrinkage. In this case, however, this mixture still showed an overall shrinkage reduction. Testing at higher dosages and higher temperatures was tried, but evaporation and/or excessive expansion did not allow for a full 120 hours of testing.

It should be reiterated that the zinc- and aluminum-based expansive agents generate hydrogen gas, which takes up space in the slurry resulting in expansion (Soucy et al., 2017). However, since chemical shrinkage testing was performed in a system open to the atmosphere, it is likely that most, if not all, of the hydrogen gas generated by the expansive agents was lost to the surroundings. This would explain the change from expansion (observed during the initial 10 hours of testing) to shrinkage in both OPC and geopolymer slurries containing the zinc- or aluminum-based expansive agents. Thus, the results presented in Figure 4.9, Figure 4.10, and Figure 4.11 may be affected by artefacts caused from testing at atmospheric pressure, suggesting that the ASTM and API shrinkage tests are not appropriate for evaluating the role of expansive agents.

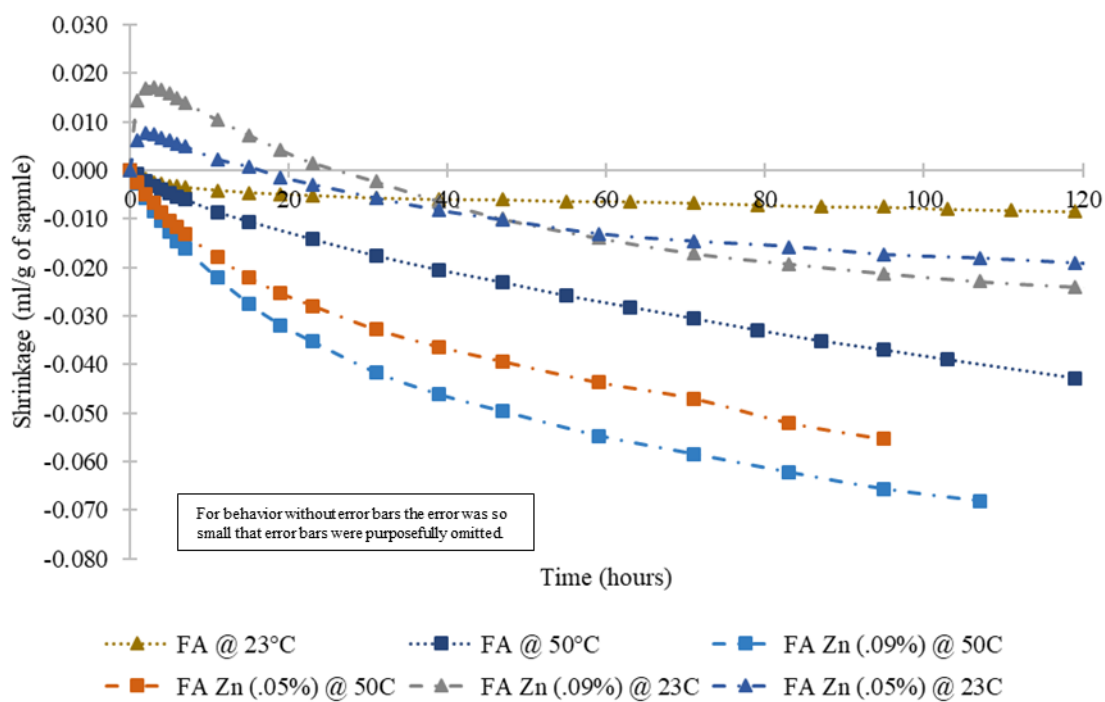


Figure 4.9: Geopolymers with zinc-based expansive agents tested at 23°C and 50°C, measured using the capillary tube test. Positive values represent sample volume expansion; negative values correspond to shrinkage.

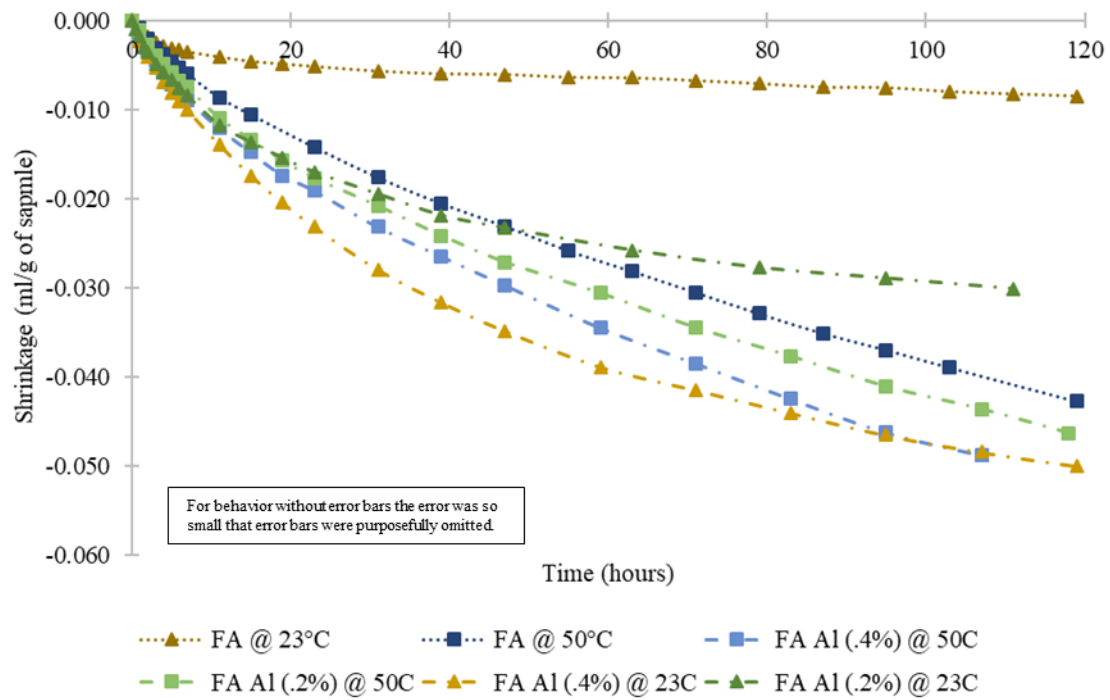


Figure 4.10: Geopolymers with aluminum-based expansive agents tested at 23°C and 50°C, measured using the capillary tube test. Positive values represent sample volume expansion; negative values correspond to shrinkage.

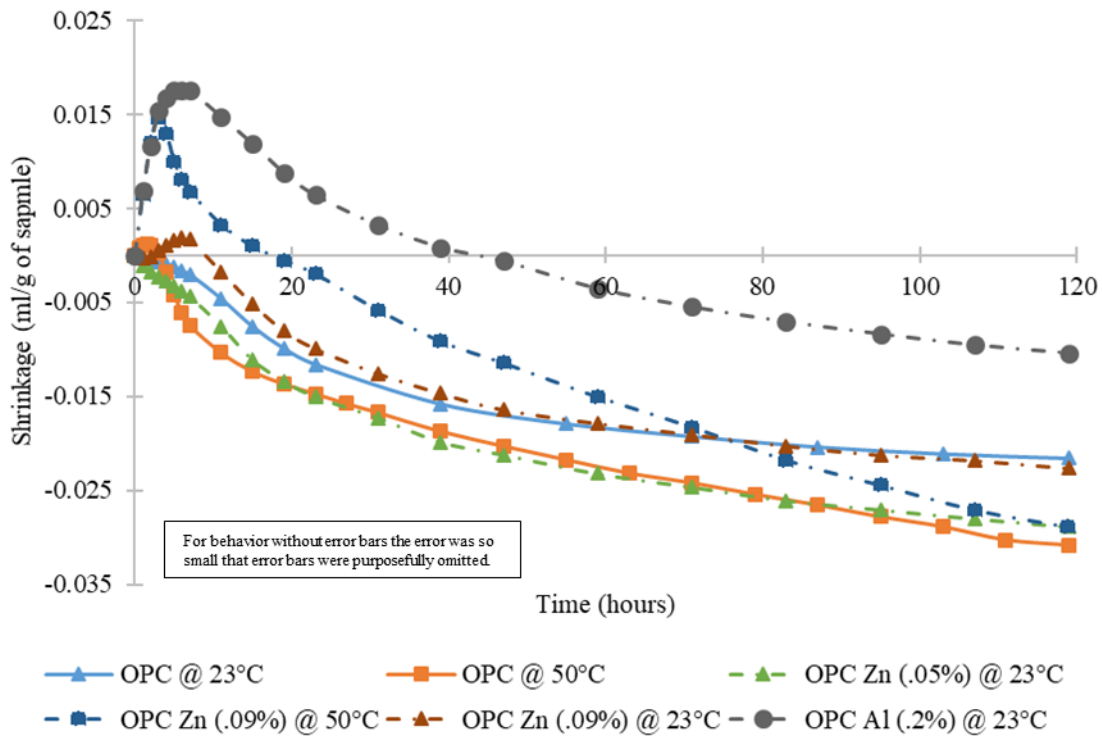


Figure 4.11: OPC with zinc- and aluminum-based expansive agents tested at 23°C and 50°, measured using the capillary tube test. Positive values indicate sample expansion; negative values correspond to shrinkage.

4.5 SHRINKAGE TESTING AT HIGH PRESSURE HIGH TEMPERATURE CONDITIONS

The standardized tests prescribed by ASTM and API allowed for shrinkage to be evaluated only at atmospheric pressure and lower temperatures. In response to these limitations, a shrinkage testing method, hereby referred to as the diaphragm accumulator test, was developed to allow for shrinkage measurements to be recorded when the samples were exposed to high temperature and high pressure. This test method allowed for evaluation of the efficacy of expansive agents in mitigating shrinkage for both geopolymer and OPC slurries which are tested at down-hole temperature and pressure conditions.

Tests on OPC and geopolymers were first run and repeated to confirm that the test method was working and was in line with what was previous discovered through the

capillary tube and membrane tests. Figure 4.12 and Figure 4.13 present the findings for OPC and geopolymer slurries tested at a pressure of 200 psi, respectively. The labeling used in the plots for diaphragm accumulator test denote the type of slurry, the test temperature, and the test pressure. For example, the label “OPC 35/200” represents the test for an OPC slurry conducted at a temperature of 35°C and pressure of 200 psi. Similarly, the label “FA + 0.09% Zn 40/2000” represents the test for geopolymer slurry containing 0.09% (by weight of cementitious material) zinc based expansive agent conducted at 40°C and 2000 psi pressure.

4.5.1 Temperature Effects

Testing on OPC slurries was originally done at 35°C and 200 psi before the diaphragm accumulator set up was changed to another heating chamber where 40°C was the low temperature setting. These temperature and pressure settings were chosen in order to maintain a constant temperature and pressure with accuracy. The results for OPC slurries, shown in Figure 4.12, confirmed that this method could measure volumetric changes in the flexible membrane with consistent and repeatable results. The observed results were as expected from a shrinkage and hydration point of view, based on the results from the capillary tube test, membrane test, and isothermal calorimetry. Increased temperature in OPC was expected to increase the rate of hydration and therefore the rate of shrinkage. With such a small difference in temperature (5°C) no significant difference in shrinkage was expected. Both of these expectations are confirmed in Figure 4.12 as the OPC mixture tested at 40°C and 200 psi confining pressure had similar observed shrinkage as the OPC mixture tested at 35°C and 200 psi confining pressure. In addition, the shrinkage development of the OPC mixture tested at 40°C and 200 psi confining pressure was slightly earlier than that of the OPC mixture tested at 35°C and 200 psi confining pressure.

After 120 hours, the total shrinkage measured in the OPC mixture tested at 40°C and 200 psi confining pressure, which will be considered the baseline test for later discussions, was 1.15%. For geopolymers a similar trend was found in terms of temperature and pressure expectations.

Geopolymers slurries were also initially tested at both 35°C and 40°C and 200 psi confining pressure using the accumulator test set-up. Figure 4.13 shows the results obtained from these tests. At 40°C and 200 psi confining pressure, the shrinkage behavior for the geopolymer slurry was similar to that of the geopolymer slurry tested at 35°C and 200 psi confining pressure. The results again confirm that increasing temperature accelerates the reaction and shrinkage, similar to the OPC and isothermal calorimetry results. In contrast to the OPC slurries, however, the geopolymer slurries did have a clear difference in total shrinkage at 120 hours despite the small 5°C difference in temperature. For the geopolymer slurry tested at 35°C and 200 psi confining pressure, the shrinkage observed was 1.95%. Meanwhile, the shrinkage in the geopolymer slurry tested at 40°C and 200 psi confining pressure was 2.63%. Though these values are different, the chemical shrinkage in the geopolymer tested at 35°C and 200 psi confining pressure appears to still be experiencing shrinkage at 120 hours whereas the geopolymer slurry tested at 40°C and 200 psi confining pressure had reached a plateau, indicating shrinkage was minimal and/or had stopped. Thus, the difference is due to a change in shrinkage rate from temperature effects. This further highlights the major effects that temperature plays on geopolymers in terms of their polymerization rate, strength, and now shrinkage. Similar to the 50°C capillary tube tests, results from the diaphragm accumulator baseline tests run at 40°C and 200 psi confining pressure show that geopolymer slurries shrink more than OPC slurries at these temperatures.

One major difference observed in the diaphragm accumulator tests, but not the capillary tube test is the presence of the inflection point previously observed in the results from isothermal calorimetry. In the cases of geopolymer slurries tested at 35°C and 200 psi confining pressure, 40°C and 200 psi confining pressure, and 80°C and 200 psi confining pressure (not yet discussed, but also in Figure 4.13), the inflection point occurred after 35, 25, and 9 hours, respectively. This result matches that of Sun and Vollpracht (2018) who also found that fly ash-based geopolymers are temperature-dependent and that increasing temperature leads to enhancement of the cumulative heat released (Sun and Vollpracht, 2018).

In terms of the inflection point itself, this could be a result of the two-stage polymerization process in fly ash geopolymers with the first stage occurring before the inflection point and the second occurring after the inflection point. Before the inflection point, the heat released could be due to the dissolution process and cause a peak in the heat release curve as the fly ash powder dissolves into the alkaline solution. Once a critical threshold is reached there is an exothermic precipitation of reaction products that results in a second peak in the rate of heat release curve and creates the observed inflection point (Sun and Vollpracht, 2018; Provis and van Deventer, 2014). In the geopolymer slurry tested at 23°C with isothermal calorimetry there was very little heat given off. This could be due to the fact that the geopolymer has not fully dissolved and precipitated at the low temperature (Sun and Vollpracht, 2018). In contrast, at 50°C the geopolymer was able to fully undergo dissolution and precipitation, leading to the presence of two peaks in the heat of polymerization curve (see Figure 4.6) and the inflection point in the cumulative heat curve (see Figure 4.8). Results from the diaphragm accumulator and isothermal calorimetry tests indicate that at 40°C/50°C the dissolution stage is short lived and produces little heat. Meanwhile the precipitation process is longer and continuous.

One of the advantages of the diaphragm accumulator test is that the temperature can be raised beyond 50°C, allowing for more representative oil well testing conditions in contrast to the capillary tube or membrane test which could only go up to 50°C and 23°C, respectively. To see the effects of temperature on the two slurry types, the baseline test conditions were raised from 40°C to 80°C while maintaining 200 psi of confining pressure. The results are presented in Figure 4.12 for an OPC slurry tested at 80°C and 200 psi confining pressure. Figure 4.13 presents a geopolymer slurry tested at 80°C and 200 psi confining pressure. The geopolymer at 80°C and 200 psi appears to have similar behavior as the baseline test conditions (40°C and 200 psi) with the two-part curve having the inflection point previously discussed being present. However, there are some key differences. With the raised temperature the rate of shrinkage was significantly faster than at 35°C/40°C. In this case the majority of the shrinkage measured comes before the inflection point (occurring after 9 hours). In addition, 2.21% total shrinkage was measured, which was actually less than that measured in the baseline test (2.63%) and was reached after just 20 hours. This suggests that at 80°C, dissolution rate increased, and more significantly, the total shrinkage was reduced in geopolymers.

For OPC, the increase in temperature to 80°C and 200 psi confining pressure caused 0.49% of shrinkage after 120 hours of testing, though the slurry had reached this shrinkage level after 20 hours, as shown in Figure 4.12. This is significantly less shrinkage than that recorded for baseline OPC tests (1.15%). This may be due to the fact that for the first 5 hours of testing, expansion was actually recorded up to a magnitude of 0.79% expansion before shrinkage began to occur for the remainder of the time measured. As seen in the isothermal calorimetry results, OPC released increasing heat when temperature was raised. Thus, the recorded expansion in the OPC slurry tested at 80°C and 200 psi was likely a

result of heat inside the flexible membrane increasing the volume of the membrane, rather than the slurry itself expanding, and taking 5 hours to stabilize. Therefore, though it would appear that OPC shrinks less when temperature is increased in the diaphragm accumulator, in contrast to capillary tube test results, the total shrinkage taken from post maximum expansion at 120 hours was 1.28%. This was greater than the shrinkage recorded with the OPC slurry at 40°C and 200 psi at 120 hours. Thus, the trend that increasing temperature results in increased shrinkage, as found with the capillary tube test, remains intact. Additional analysis taking into account thermal expansion was not performed in this study but is recommend for future studies to understand the full behavior of the slurry in question.

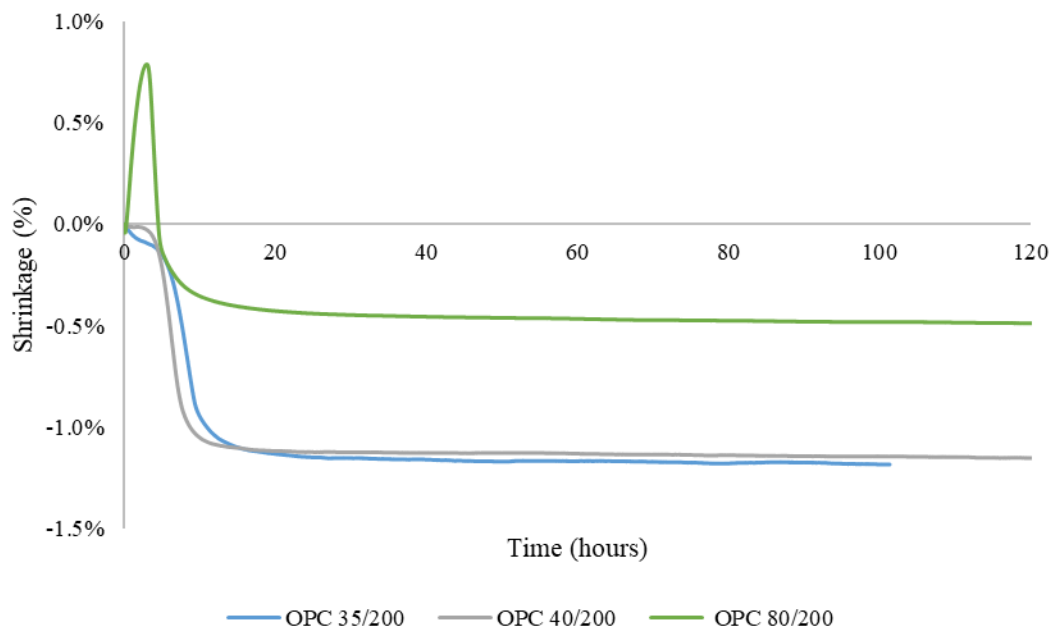


Figure 4.12: OPC shrinkage at 200 psi and 40°C or 80°C, measured using the diaphragm accumulator test.

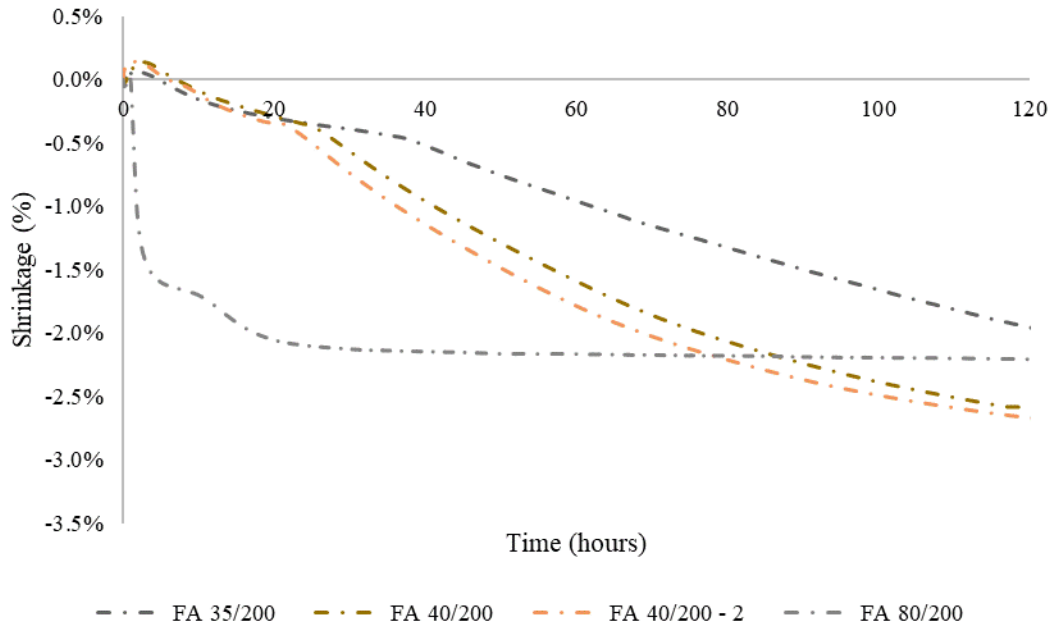


Figure 4.13: Geopolymer shrinkage at 200 psi and 35°C, 40°C, or 80°C, measured using the diaphragm accumulator test.

4.5.2 Effects of Expansive Agents

The efficacy of zinc- and aluminum-based expansive agents to mitigate shrinkage in OPC and geopolymer slurries was not accurately captured using standardized testing methods. The diaphragm accumulator tests were carried out at pressures of 200 psi or greater to prevent the loss of hydrogen gas produced by the expansive agents.

4.5.2.1 Effect of Expansive Agents on OPC Slurries

Figure 4.14 and Figure 4.15 show the shrinkage measured using the accumulator test method on OPC slurries containing zinc- and aluminum-based expansive agents, respectively. The zinc-based expansive agent was added to OPC slurries at a dosage of 0.09% (by weight) and tested at a pressure of 200 psi and either 40°C or 80°C. For an OPC slurry with zinc-based expansive agent tested at 40°C and 200 psi confinement, the total

shrinkage after 120 hours was 0.88%, which is 23.5% less than that observed for OPC slurry without expansive agent tested at the same temperature and pressure condition. This indicates that the addition of zinc-based expansive agent was successful in mitigating shrinkage in OPC slurries. When tested at 80°C and 200 psi confining pressure, the OPC slurry with zinc-based expansive agent experienced 0.94% expansion over the first 4 hours of measurement before shrinking a total of 0.08% after 120 hours. The shrinkage measured after peak expansion was 1.02%, which is less than that recorded for the OPC slurry (without expansive agent) at 80°C and 200 psi confining pressure (1.28%). This further demonstrates that the inclusion of zinc-based expansive agents reduced shrinkage in OPC slurries when tested at elevated temperature and pressure conditions.

Aluminum-based expansive agent was added to the OPC slurries at a 0.4% (by weight) dosage and also tested at 200 psi and either 40°C or 80°C (see Figure 4.15). Expansive behavior characterized the first 5 hours of the OPC slurry with aluminum-based expansive agent tested at 40°C and 200 psi up to a magnitude of 1.85% before shrinkage began. In this case, however, there was 1.15% shrinkage after the maximum expansion, and after 120 hours a net volume increase was recorded (0.70% expansion at 120 hours). The shrinkage after maximum expansion was equal to the total shrinkage measured in the OPC slurry without the expansive agents, which would suggest that the expansive agent did not help. In contrast to the baseline mix, however, this mix had a net positive volume change after 120 hours, which means that although the total measured shrinkage was the same, the sample still had a positive volume response overall. Similarly, the OPC slurry with aluminum-based expansive agent tested at 80°C and 200 psi experienced expansion for the first 5 hours up to magnitude of 1.40% before 0.81% shrinkage began. The total volume change at 120 hours in this mix was 0.59%. In this case the shrinkage after maximum expansion was less than that observed in the OPC slurry tested at 80°C and 200

psi, and a net volume increase occurred after the 120-hour test period. Therefore, at the elevated temperature, the addition of the aluminum expansive agent aided in shrinkage mitigation as well.

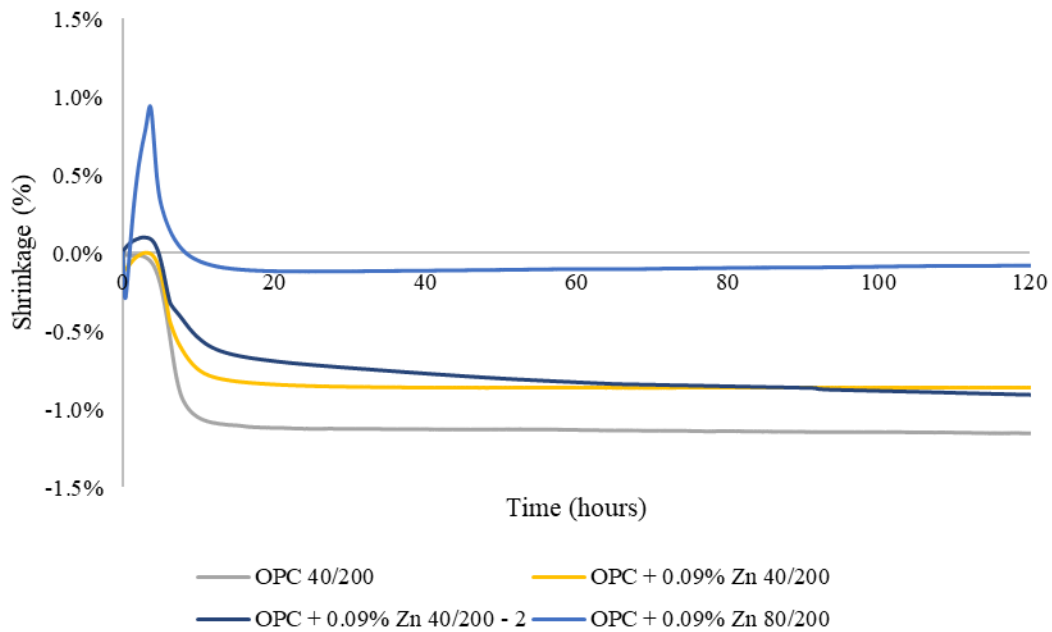


Figure 4.14: OPC shrinkage with zinc-based expansive agent at 200 psi and 40°C or 80°C, measured using the diaphragm accumulator test.

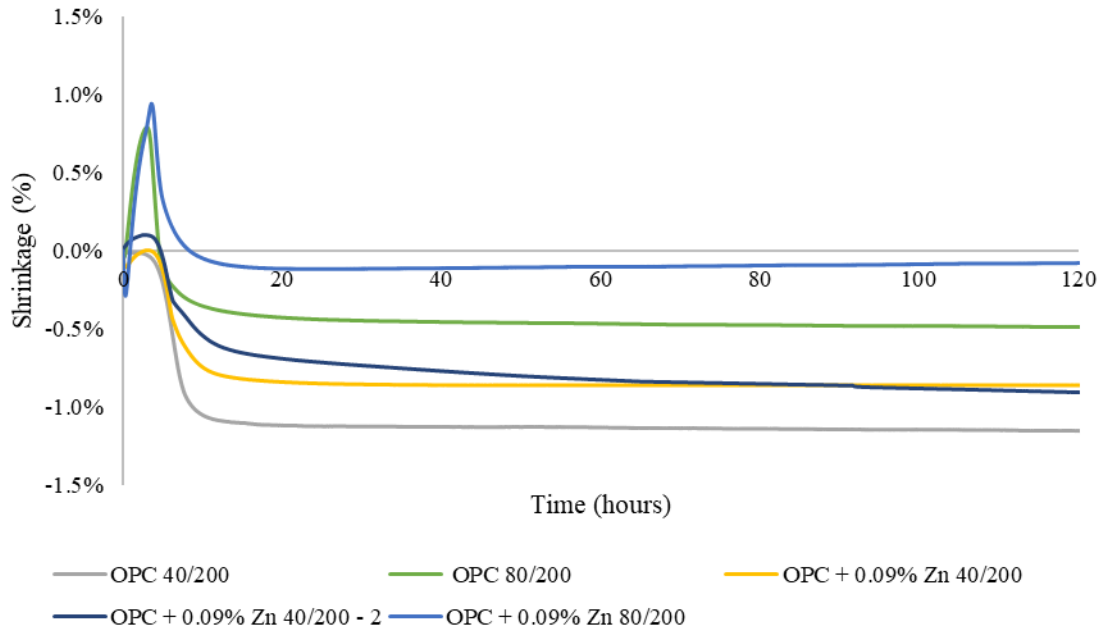


Figure 4.15: OPC shrinkage with 0.4% Aluminum expansive agent at 200 psi and 40°C or 80°C, measured using the diaphragm accumulator test.

4.5.2.2 Effect of Expansive Agents on Geopolymer Slurries

For geopolymers, the same dosages of expansive agents (0.09% zinc; 0.4% aluminum) were applied and tested. Results for geopolymer mixes with zinc-based expansive agent at 40°C, zinc-based expansive agent at 80°C, and aluminum-based expansive agents are presented in Figure 4.16, Figure 4.17, and Figure 4.18, respectively. While there was some expansion observed in the early stages of testing (similar to OPC), the expansive values were small compared to those recorded with OPC. Therefore, for the purposes of discussion, the expansive behavior observed will be considered negligible, and only shrinkage at 120 hours of testing will be discussed.

In the geopolymer with zinc-based expansive agent tested at 40°C and 200psi, the total shrinkage observed was 2.61%. This was very close to the shrinkage recorded for geopolymers (without expansive agents) tested at 40°C and 200 psi confining pressure

(2.63%). In addition, the location of the inflection point and the rate of shrinkage recorded for geopolymer slurries with zinc-based expansive agent was similar to that for plain geopolymer slurries (i.e. geopolymer slurries without expansive agents). However, the addition of zinc-based expansive agent to geopolymer slurries that were tested at 80°C and 200 psi confining pressure reduced the total shrinkage recorded after 120 hours from 2.21% to 1.37%. This indicates that the addition of zinc-based expansive agents has the potential to mitigate shrinkage in geopolymers, particularly at higher temperatures.

However, increasing the dosage of the zinc-based expansive agent to 0.2% (by weight of fly-ash) resulted in higher shrinkage (2.37%) than that recorded for plain geopolymers (i.e. geopolymers without expansive agent) (2.21%) tested at 80°C and 200 psi confining pressure (see Figure 4.17). Therefore, further investigation needs to be conducted to arrive at optimum dosage of the zinc-based expansive agents to mitigate shrinkage in geopolymer systems subjected to 80°C and 200 psi confining pressure.

The addition of 0.4% (by weight of fly ash) aluminum-based expansive agent to the geopolymer slurry resulted in a 12.5% increase in the total shrinkage recorded at 120 hours of testing at 40°C and 200 psi confining pressure. Furthermore, geopolymers containing aluminum-based expansive agent showed a similar rate of shrinkage as geopolymers without expansive agent, but the shrinkage occurred 2.5 hours earlier. These results demonstrate that the aluminum-based expansive agent does not mitigate shrinkage for the geopolymers evaluated during this study at the dosage tested.

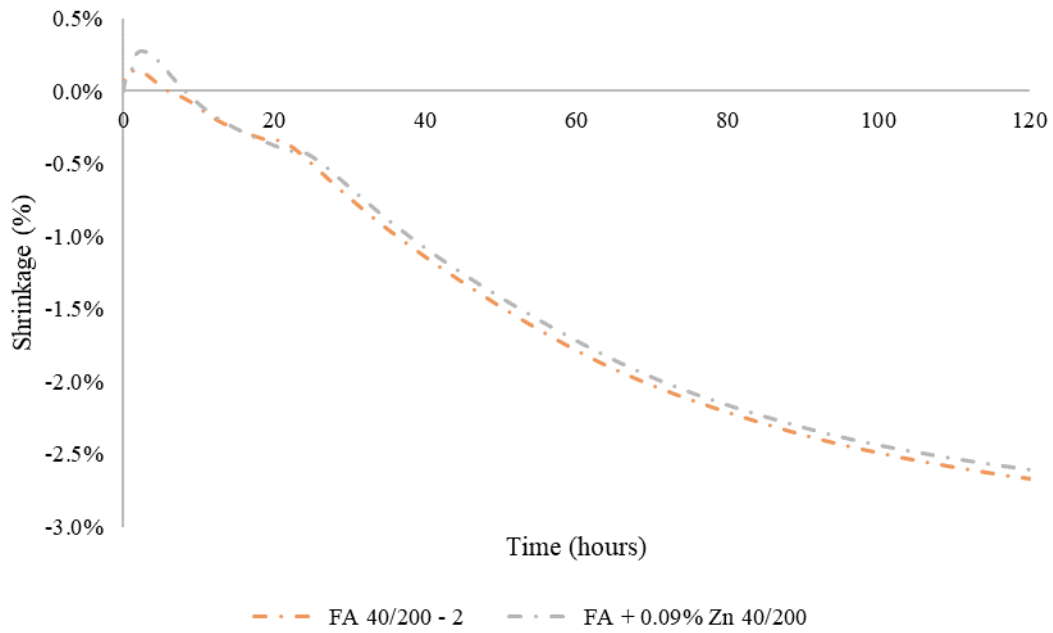


Figure 4.16: Geopolymer shrinkage with zinc-based expansive agent at 40°C and 200 psi, measured using the diaphragm accumulator test.

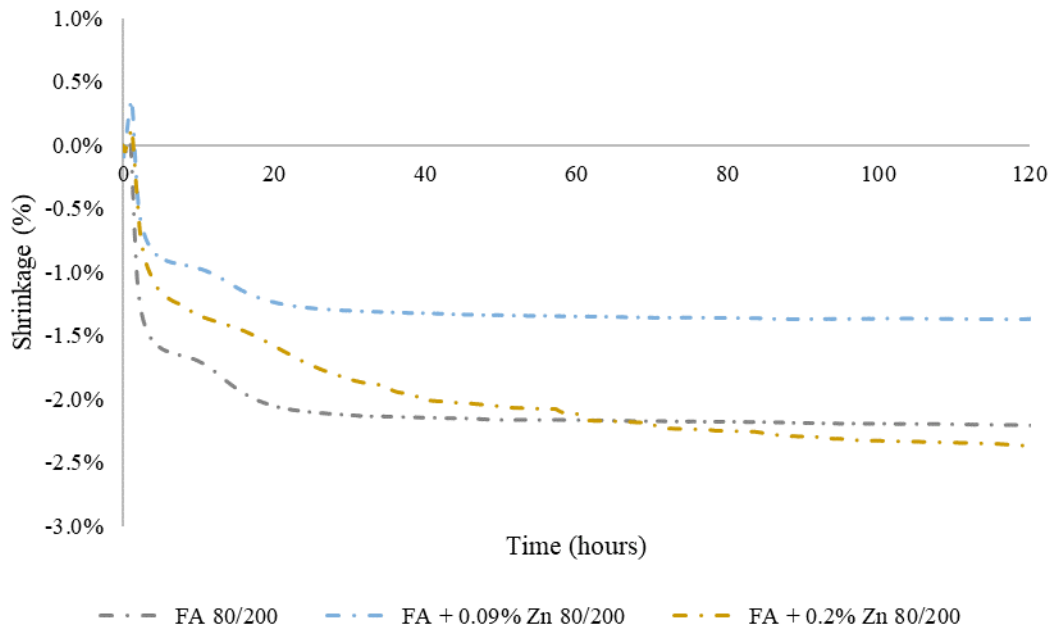


Figure 4.17: Geopolymer shrinkage with zinc-based expansive agent at 80°C and 200 psi, measured using the diaphragm accumulator test.

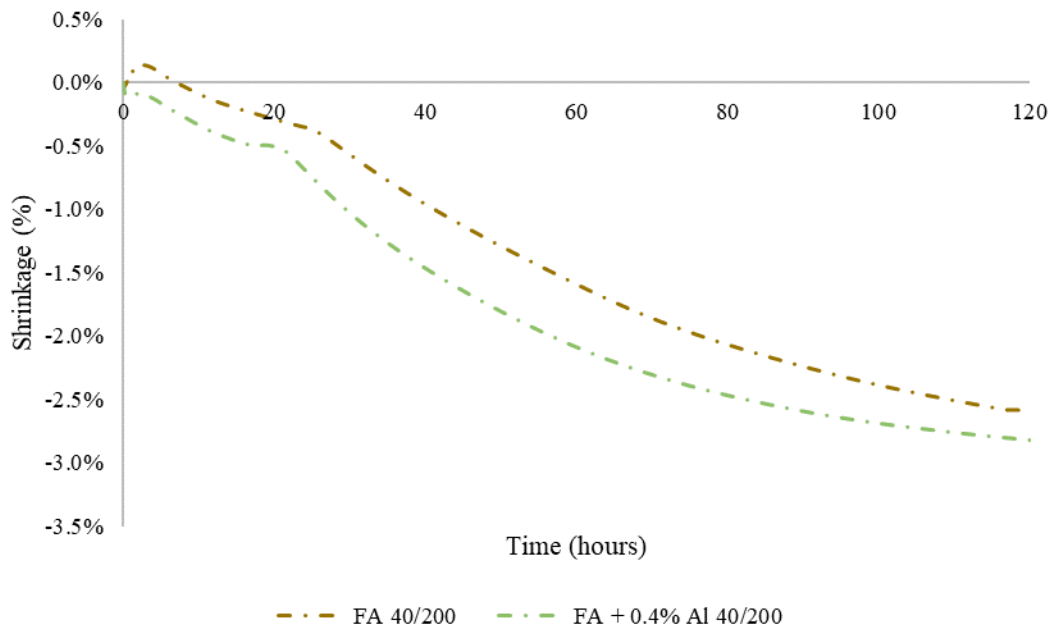


Figure 4.18: OPC shrinkage with zinc-based expansive agent at 200 psi and 40°C or 80°C, measured using the diaphragm accumulator test.

4.5.3 Effects of Elevated Pressure

In addition to the ability to increase the test temperature, pressure can also be raised up to 2000 psi with the diaphragm accumulator test set up. The following discussion involves testing of an OPC slurry at 40°C and 2000 psi, an OPC slurry with either 0.09% zinc-based expansive agent or 0.4% aluminum-based expansive agent at 40°C and 2000 psi, and a geopolymer slurry at 40°C and 2000 psi. The results for these tests are presented in Figure 4.19, Figure 4.20, and Figure 4.21, respectively. Note, there are two tests (a geopolymer tested at 40°C and 2000 psi and an OPC slurry with 0.4% aluminum-based expansive agent tested at 40°C and 2000 psi) where there was a linear, zero slope shrinkage behavior observed. This is due to the test system running out of oil to pump into the accumulator, rather than the actual shrinkage behavior of the sample. Should this issue not

have arisen, the behavior after observed zero slope would be shifted earlier in time to reach the point in time where the problem started.

When temperature was maintained at 40°C and the pressure raised from 200 psi to 2000 psi, the total shrinkage in the OPC slurry increased from 1.15% to 3.26% at 120 hours, as seen in Figure 4.19. When zinc- and aluminum-based expansive agents were added (at a dosage of 0.09% and 0.4%, respectively) to OPC slurries and tested at 40°C and 2000 psi, the total shrinkage after 120 hours was found to be 2.99% and 1.92%, respectively. This behavior is seen in Figure 4.20. These results prove that the addition of these expansive agents does in fact provide shrinkage mitigation. At this elevated pressure condition, the OPC mix with aluminum-based expansive agent performed better, though it did have a much larger dosage, which may have helped its performance. When the geopolymer slurry was tested at the elevated 2000 psi pressure and 40°C, as seen in Figure 4.21, the total shrinkage measured after 120 hours was 2.85%. This is less than a 10% increase in shrinkage compared to the geopolymer slurry at 40°C and 200 psi confining pressure.

The results from the raised pressure conditions indicate that there is a correlation between pressure and total shrinkage experienced in both OPC and geopolymers. At relatively low temperatures and pressures (40°C and 200 psi) OPC was much more stable than geopolymers in terms of total shrinkage (1.15% shrinkage as opposed to 2.63%). When tested at high pressures, the OPC lost this shrinkage stability and was much more sensitive to pressure changes than geopolymers. This sensitivity is so high that at the higher pressures the OPC slurry experienced more shrinkage than the geopolymer slurry. The use of 0.09% zinc- and 0.4% aluminum-based expansive agents in the OPC helped reduce the total shrinkage at higher pressures, as seen in Figure 4.20, but only the 0.4% aluminum-

based expansive agent-containing mixture managed to have less shrinkage than the geopolymer at the elevated pressure.

Testing on geopolymers with expansive agents at 40°C and 2000 psi, OPC/geopolymers at 80°C and 2000 psi, and OPC/geopolymers with expansive agents at 80°C and 2000psi was not performed, but it is inferred that the previously discussed trends would hold true. That is, for OPC, increasing temperature would increase the shrinkage observed. For geopolymers with zinc-based expansive agents there would be shrinkage reduction compared to neat geopolymer slurries, but for geopolymers with aluminum-based expansive agents there would be equal or more shrinkage observed. In addition, raising the temperature on the geopolymer actually helped reduce shrinkage as seen by the geopolymer tested at 80°C and 200psi. It would thus be expected that the combination of increased pressure and temperature (80°C and 2000psi) in geopolymers would result in similar results to that of the geopolymer baseline tests (40°C and 200psi). The addition of zinc-based expansive agent would then help in reducing the resulting shrinkage.

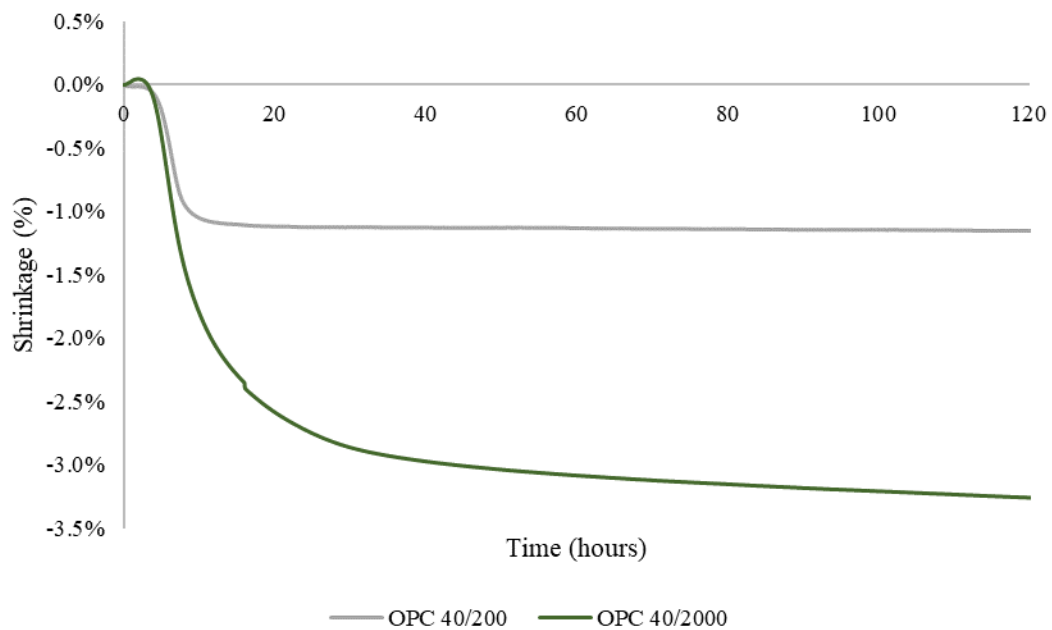


Figure 4.19: OPC shrinkage at 2000 psi and 40°C, measured using the diaphragm accumulator test.

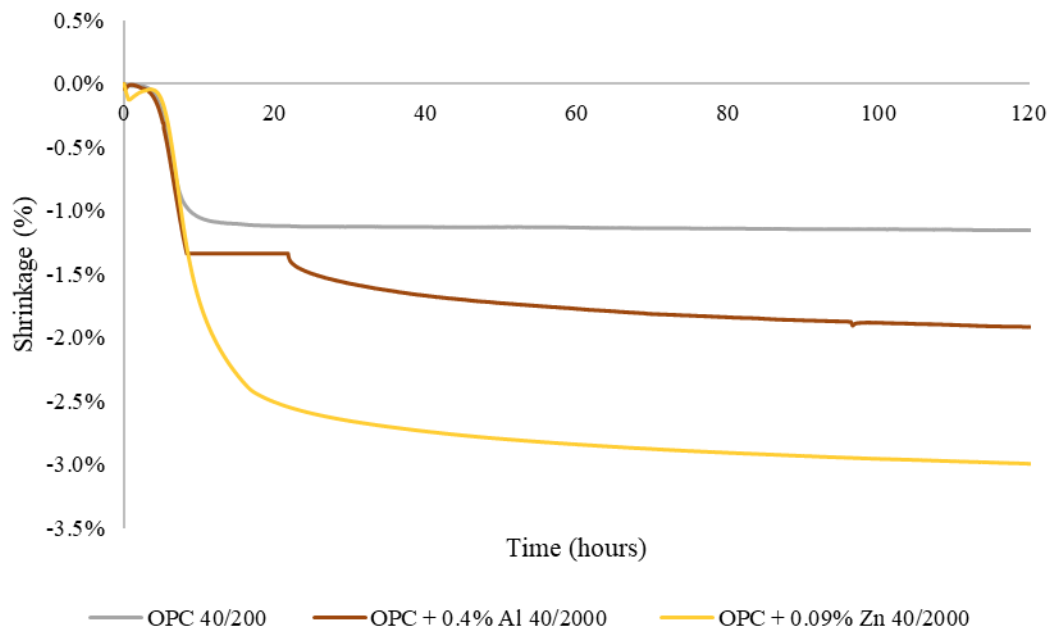


Figure 4.20: OPC shrinkage with zinc- and aluminum-based expansive agents at 2000 psi and 40°C, measured using the diaphragm accumulator test.

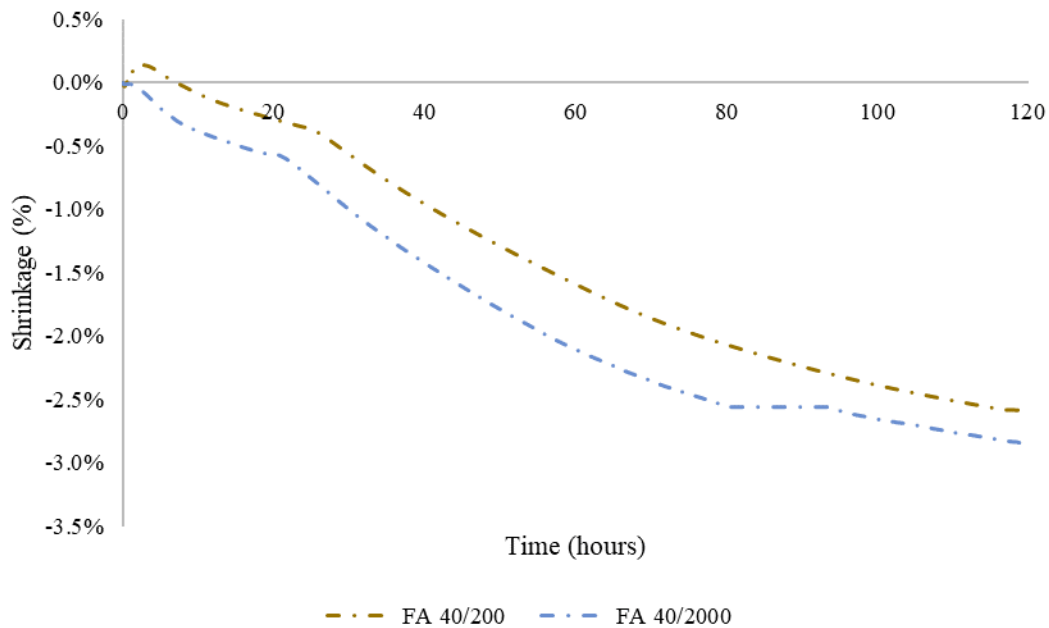


Figure 4.21: Geopolymer shrinkage at 2000 psi and 40°C, measured using the diaphragm accumulator test.

4.6 OPTICAL MICROSCOPE IMAGING

Optical microscope imaging was conducted on OPC and geopolymer samples with and without zinc- or aluminum-based expansive agents to document the impact of expansive agents on the microstructure of hardened cement. Figure 4.22 shows images of the cross-section taken for an OPC sample with no expansive agent at 40°C and 200 psi. Figure 4.23 and Figure 4.24 presents the images taken of the cross-section of OPC samples with aluminum- and zinc-based expansive agent, respectively.

As shown in Figure 4.22-1a there are a few sporadic pockets of air voids in the OPC cross-section, but these are likely due to insufficient agitation of the slurry. Upon closer examination under a microscope, Figure 4.22-1b and Figure 4.22-1c, the sample does show small air voids (visible as white or dark gray spots on the sample), but these voids are small and well distributed throughout the cross-section. When expansive agents are added,

however, the presence of air voids becomes prevalent. Regardless of whether zinc- or aluminum-based expansive agent was used, it was observed that increasing temperature resulted in larger, but fewer air voids and that increasing pressure resulted in smaller and fewer voids. Specifically, OPC samples tested at 80°C and 200 psi had larger voids (in terms of size) than OPC samples tested at 40°C and 200 psi. However, the quantity of air voids was reduced. When OPC samples were tested at 40°C and 2000 psi, the size of air voids was about the same (if not smaller) as that of OPC samples at 40°C and 200 psi, however, in this case the number of voids is fewer. From these results, it is thus found that the use of expansive agents will in fact produce air voids from the creation of hydrogen which is what aids in shrinkage mitigation. In addition, the distribution of air voids on the cross-section was not quite even, but the voids were spread out.

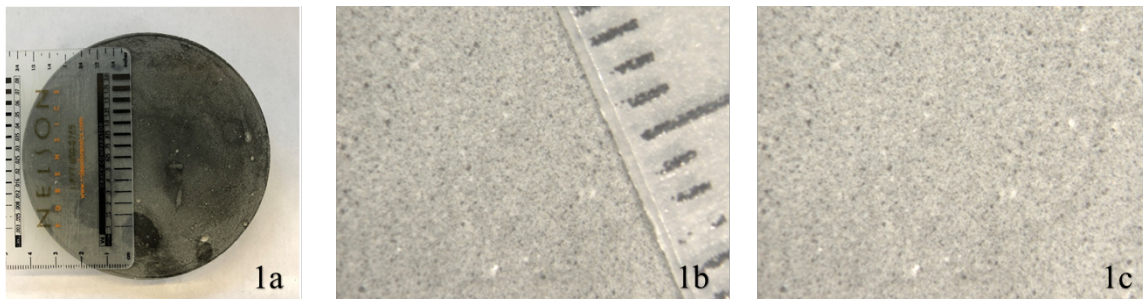


Figure 4.22: OPC sample tested at 40°C and 200 psi. Optical microscope images (b and c) taken at 0.8X magnification.

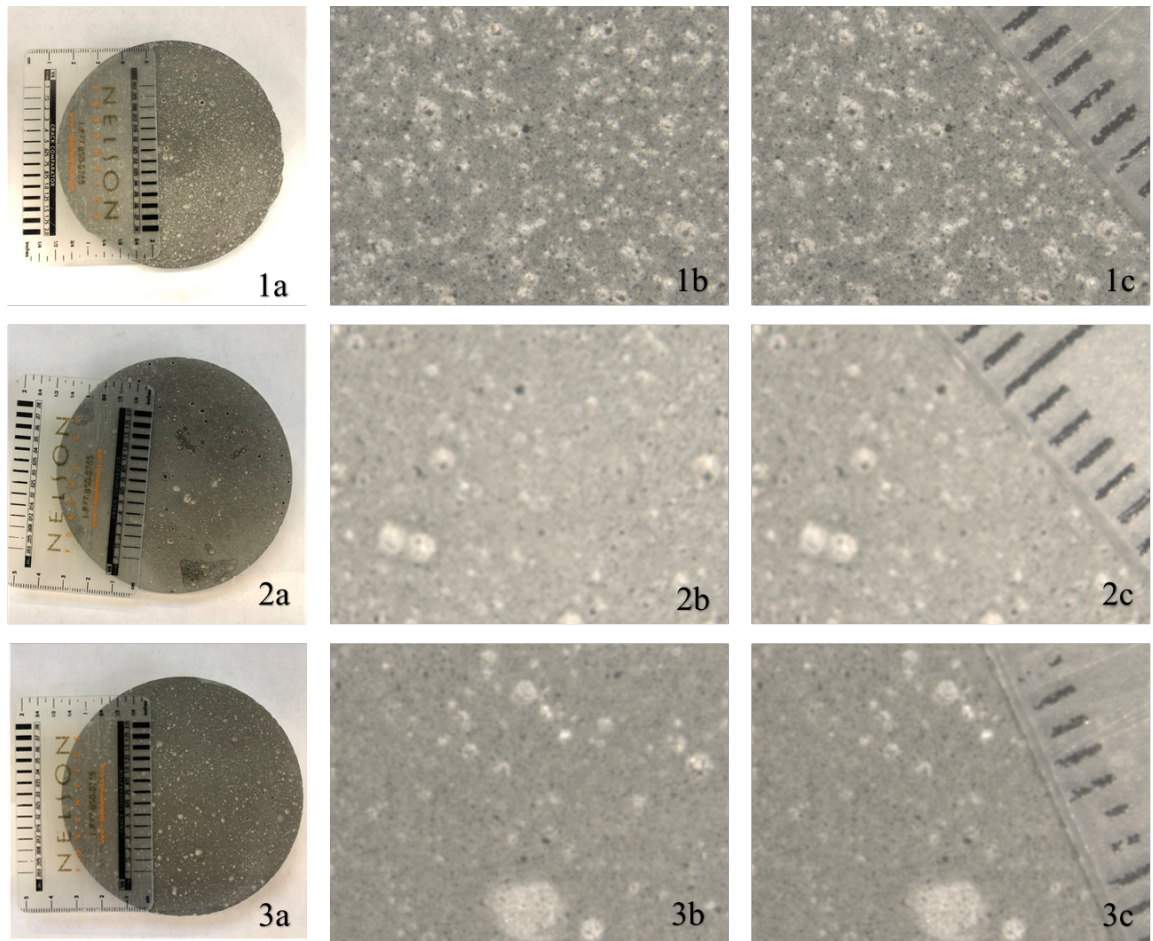


Figure 4.23: OPC samples with 1) 0.4% aluminum-based expansive agent at 40°C and 200 psi. 2) 0.4% aluminum-based expansive agent at 80°C and 200 psi. 3) 0.4% aluminum-based expansive agent at 40°C and 2000 psi. Optical microscope images (b and c) taken at 0.8X magnification.

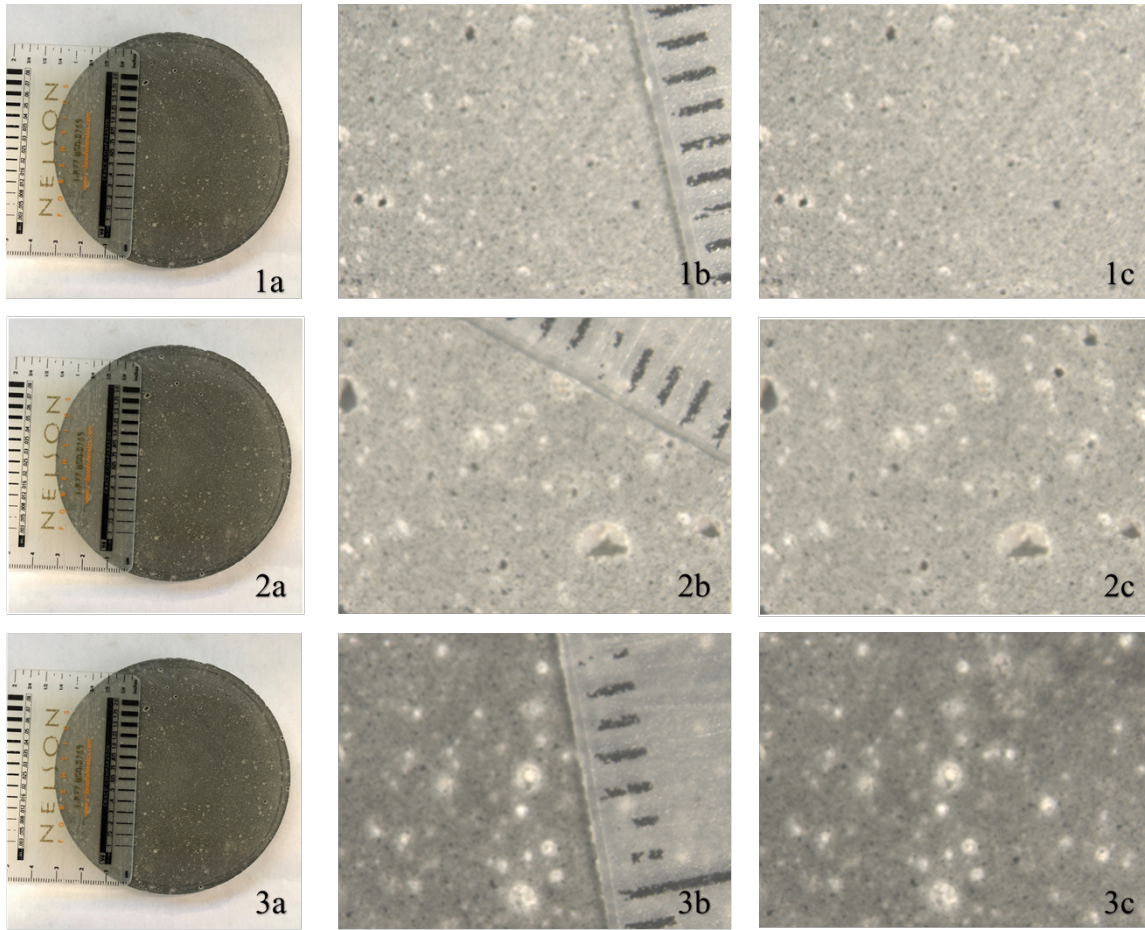


Figure 4.24: OPC samples with 1) 0.09% zinc-based expansive agent at 40°C and 200 psi. 2) 0.09% zinc-based expansive agent at 80°C and 200 psi. 3) 0.09% zinc-based expansive agent at 40°C and 2000 psi. Optical microscope images (b and c) taken at 0.8X magnification.

CHAPTER 5 : CONCLUSIONS AND FUTURE WORK

Previous studies on low calcium alkali-activated materials (geopolymers) have shown that they have adequate strength, rheological properties, and setting time to be used for oil well cementing (Aughenbaugh et al.; 2014; Liu et al., 2016; Liu, 2017). Most importantly, geopolymers have been proven to have greater compatibility with NAFs than OPC (Liu et al., 2016; Liu, 2017). In particular, geopolymers/geopolymer-hybrids prepared using Class F fly ash and 8M sodium hydroxide and containing up to 40% SBM (by volume) have been shown to have the desired strength, viscosity, and thickening time properties required for different oil well cementing applications. However, the shrinkage behavior of these geopolymers and geopolymer-hybrids remained to be studied before recommending them for field application. Therefore, the goal of this research was to characterize the shrinkage behavior of geopolymer (prepared using Class F fly ash and 8M sodium hydroxide) and geopolymer-hybrid systems. Shrinkage was evaluated at different curing temperatures, pressures, and SBM contamination levels. In addition, a shrinkage mitigation technique using zinc- and aluminum- based expansive agents was also explored for both OPC and geopolymer systems.

In this thesis, an overview of the formulations, advantages, and application of geopolymers into the field of oil was presented in Chapter 2. A description of the materials and experimental methods employed in this study were provided in Chapter 3. Chapter 4 evaluated the behavior of the geopolymers and geopolymer-hybrids and compared them to OPC systems. Finally, this chapter lists the significant conclusions found from this study and presents suggestions for future work.

5.1 CONCLUSIONS

The early-age shrinkage behavior of Class H OPC and Class F fly ash activated by a 8M sodium hydroxide-based geopolymer slurries was characterized at different temperatures (23°C, 40°C, 50°C, 80°C), SBM contamination levels (0%, 10%, and 20% by volume), and applied pressures (200 psi and 2000 psi). The effects of zinc- and aluminum-based expansive agents on shrinkage behavior by the OPC and geopolymer slurries was also explored as a possible shrinkage mitigation technique. Through the use of existing standardized test methods and a novel shrinkage test designed specifically to measure the effect of pressure on shrinkage, the following conclusions were reached:

- At room temperature (23°C), geopolymer and geopolymer-hybrid systems appear to shrink significantly less than OPC slurries. This, however, is a result of the low rate of reaction/polymerization at room temperature. Isothermal calorimetry confirms that there is very little heat released when geopolymer slurries are tested at room temperature, and visual observations of slurries at 120 hours confirm that the slurry was not hardened.
- At higher temperatures and low-pressure conditions (40°C/200psi, 50°C/0psi, and 80°C/200psi), geopolymers shrank more than OPC slurries.
- For OPC, there was a positive correlation between temperature and shrinkage regardless of pressure, as there was a greater rate and degree of hydration occurring at higher temperatures. That is, as temperature increased, so did shrinkage. These results confirm concerns about shrinkage interfering with zonal isolation in oil and gas well cementing applications, which are characterized by high temperature high pressure conditions.
- In geopolymers, there was a positive correlation between temperature and shrinkage at atmospheric conditions as seen by testing at 23°C and 50°C with the

capillary tube test. However, under pressurized testing with the diaphragm accumulator, this trend seemed to be reversed when comparing geopolymer results at 40°C/200psi and 80°C/200psi. That is, the geopolymer tested at 80°C and 200psi had less shrinkage than the geopolymer tested at 40°C and 200psi. Though the geopolymer still experienced more shrinkage at these conditions than OPC slurry, the results suggest that increasing temperature beyond 80°C may lead to less shrinkage in geopolymers than OPC.

- Contamination with SBM increased the shrinkage tendencies in both OPC and geopolymer slurries, as seen by capillary tube test results. A geopolymer slurry with 10% SBM (by volume) shrank less than an OPC slurry contaminated with 10% SBM (by volume) when tested at 50°C.
- When tested with existing industry standard methods, OPC and geopolymers with zinc- or aluminum-based expansive agents showed potential to be effective additives for shrinkage mitigation.
- The work conducted in this research exposed limitations in using standardized testing methods to evaluate shrinkage. Specifically, the membrane test can only be run at atmosphere pressure and is limited to a temperature of 23°C due to issues with membrane melting. The capillary tube test is limited to atmospheric pressure and a temperature of 50°C before issues with evaporation of water begin to produce artefacts in the results. Additionally, the use of exothermic reacting expansive agents (such as the zinc- and aluminum-based expansive agents used in this study) is not recommended in the capillary tube test. Unless the dosage is quite small, it was found that expansion effects can cause the capillary tube to overflow and that there are artefacts in measured data due to loss of hydrogen gas to the atmosphere.

- The inability of the testing methods described in ASTM C1608-18 and API 10B-5 / ISO 14026-5 to test at elevated temperatures and apply confining pressure, as is the case in well conditions, were eliminated through the use of the diaphragm accumulator test method. Shrinkage could be accurately measured at temperatures of 35 – 80°C and at pressures of 200 – 2000 psi using the diaphragm accumulator test setup. The test set-up can be easily modified to measure shrinkage at higher temperatures and pressures by using the appropriate type of hydraulic pump, oven, and accumulator. The diaphragm accumulator test allows for real time measurements with 0.02% accuracy. Furthermore, this test set-up was able to accurately measure the impact of zinc- and aluminum-based expansive agents on shrinkage mitigation of OPC and geopolymer slurries.
- The use of expansive agents, such as zinc- and aluminum-based expansive agents are effective shrinkage mitigation additives, particularly at high pressures,
 - The addition of 0.4% aluminum-based expansive agent is effective for shrinkage mitigation in OPC at 40°C/200psi, 80°C/200psi, and 40°C/2000psi causing net expansion in the first two conditions but making no significant difference in geopolymers at 40°C/200psi.
 - The addition of 0.09% zinc-based expansive agent is effective for mitigating shrinkage in OPC slurries tested at 40°C/200 psi, 80°C/200 psi, and 40°C/2000 psi. For geopolymers slurries, the addition of 0.09% zinc-based expansive agent reduced shrinkage when tested at 40°C/200psi and 80°C/200 psi. The addition of aluminum-based expansive agents failed to reduce shrinkage in geopolymers, therefore the zinc-based expansive agent is the better suited additive for geopolymer systems tested during this study.

- Photographs from optical microscopic imaging further confirm the effectiveness of zinc- and aluminum-based expansive agents through the presence of air voids. In samples without expansive agents, there was almost no presence of air voids. When the expansive agents were introduced voids became prevalent. In OPC samples, the increase in temperature resulted in larger, but fewer air voids. This trend was observed by comparing OPC samples with zinc- or aluminum-based expansive agent tested at 80°C and 200 psi confining pressure with OPC samples with zinc- or aluminum-based expansive agent tested at 40°C and 200 psi. Furthermore, increasing pressure in OPC samples resulted in similarly sized (if not smaller) and fewer air voids. This was observed by comparing OPC samples with zinc- or aluminum-based expansive agent tested at 40°C and 200 psi confining pressure with OPC samples with zinc- or aluminum-based expansive agent tested at 40°C and 2000 psi.
- In geopolymers, increasing pressure from 200 psi to 2000 psi at 40°C only slightly increased shrinkage, indicating that pressure effects, though still increasing shrinkage, are minor in the geopolymer formulations. Meanwhile, for OPC the same increase caused a significant increase in shrinkage (almost 3x that of OPC at 40°C/200psi) and the shrinkage exceeded that observed in geopolymers.

Overall, it was seen that increased temperature, contamination, and pressure were increasing shrinkage in both OPC and geopolymers. The results confirm the concern regarding OPC shrinkage effects interfering with achieving proper zonal isolation. In addition, the results proved that geopolymers may be a suitable alternative as an oil and gas well cementing material at elevated temperatures and pressures. If the observed trends hold, it is inferred that a geopolymer would develop less shrinkage than an OPC slurry tested under true oil and gas well conditions. If this is true, geopolymers would truly be

more effective and superior to OPC as a cementing material as it would then be proven that geopolymers have:

- Adequate/superior strength in neat and contaminated slurries
- Better compatibility with NAF drilling muds allowing NAF solidification
- Superior rheological properties when SBM is added to the mix
- Reduced shrinkage at elevated temperature and pressures

5.2 RECOMMENDATIONS FOR FUTURE WORK

The following are suggestions and/or recommendations for future work on evaluating the shrinkage of geopolymers:

- Further testing with the diaphragm accumulator test on OPC and geopolymers at 80°C/2000psi or higher is recommended. These test conditions provide the most realistic simulation of downhole conditions and would confirm the effectiveness of the geopolymer prepared using Class F fly ash and 8M sodium hydroxide over OPC.
- Shrinkage testing on geopolymers prepared using silicate-based activating solutions is recommended.
- Alternate dosages of the zinc- and aluminum-based expansive agents in OPC and geopolymers should be tested using the diaphragm accumulator test. The objective of this testing would be to optimize the dosage of expansive agent for each mixture depending on curing conditions (i.e. temperature and confining pressure). Specifically, it is recommended to test zinc-based expansive agents at dosages ranging from 0.2% to 2% (by weight). Aluminum-based expansive agents should be tested at a dosage range of 0.8% to 2% (by weight).

- Geopolymers should be tested in an apparatus that allows for concurrent measurement of total volume changes, but also bulk volume changes at realistic oil and well conditions. This testing would allow for an understanding of not only the external confining pressures (as is the case in the diaphragm accumulator), but also the (internal) pore pressure acting on the sample.

REFERENCES

- API 10B-5, 2015. Recommended Practice on Determination of Shrinkage and Expansion of Well Cement Formulations at Atmospheric Pressure.
- API RP 10B-2, 2010. Recommended Practice for Testing Well Cements.
- ASTM C311-13, 2013. Standard Test Methods for Sampling and Testing Fly Ash or Natural Pozzolans for Use in Portland Cement Concrete.
- ASTM C845-18, 2018. Standard Specification for Expansive Hydraulic Cement.
- ASTM C618-17, 2017. Standard Specification for Coal Fly Ash and Raw or Calcined Natural Pozzolan for Use in Concrete.
- ASTM C1608-17, 2017. Standard Test Method for Chemical Shrinkage of Hydraulic Cement Paste.
- ASTM C1679-17, 2017. Standard Practice for Measuring Hydration Kinetics of Hydraulic Cementitious Mixtures Using Isothermal Calorimetry.
- Atiş, C. D., Bilim, C., Çelik, Ö, and Karahan, O., 2009. Influence of activator on the strength and drying shrinkage of alkali-activated slag mortar. *Construction and Building Materials*, 23(1), 548-555. doi:10.1016/j.conbuildmat.2007.10.011
- Aughenbaugh, K.L., 2013. Fly ash-based Geopolymers: Identifying Reactive Glassy Phases in Potential Raw Materials
- Aughenbaugh, K.L., Nair, S.D., Cowan, K., van Oort, E., 2014. Contamination of Deepwater Well Cementations by Synthetic-Based Drilling Fluids, in: SPE Deepwater Drilling and Completions Conference. Galveston, TX. doi:10.2118/170325-MS. 12
- Bakharev, T., Sanjayan, J., & Cheng, Y., 1999. Effect of elevated temperature curing on properties of alkali-activated slag concrete. *Cement and Concrete Research*, 29(10), 1619-1625. doi:10.1016/s0008-8846(99)00143-x
- Beach, H.J., Goins, W.C.J., 1957. A Method of Protecting Cements Against the Harmful Effects of Mud Contamination. *Petroleum Transactions, AIME*, Volume 210, 148-152.
- Brooks, J. J., 2015. Concrete and masonry movements. Amsterdam: Elsevier.
- Brooks, J. J., 2000. Elasticity, creep and shrinkage of concrete containing admixtures. In: Al-Manaseer Akthem, editor. *Proceedings Adam Neville symposium: creep and shrinkage – structural design effects*. Atlanta: ACI Special Publication SP – 194; 1997, 2000. pp. 283-360.
- Carter, L., Waggoner, H., & George, C., 1966. Expanding Cements for Primary Cementing. *Journal of Petroleum Technology*, 18(05), 551-558. doi:10.2118/1235-pa

- Chen, W., Brouwers, H., 2007. The hydration of slag, part 1: reaction models for alkali-activated slag. *J. Mater. Sci.* 42 (2), 428–443
- Copeland, L. E., & Bragg, R. H., 1955. Self-desiccation in Portland cement pastes. Chicago: Portland Cement Association.
- Davidovits, J., 1989. Geopolymers: Inorganic Polymeric New Materials. Presented at the Symposium on Chemical Thermodynamics, Calorimetry and Thermal Analysis 1989, pp 1633-1656.
- Duxson, P., Fernández-Jiménez, A., Provis, J. L., Lukey, G. C., Palomo, A., & Deventer, J. S., 2006. Geopolymer technology: The current state of the art. *Journal of Materials Science*, 42(9), 2917-2933. doi:10.1007/s10853-006-0637-z
- Duxson, P., Mallicoat, S., Lukey, G., Kriven, W., & Deventer, J. V., 2007. The effect of alkali and Si/Al ratio on the development of mechanical properties of metakaolin-based geopolymers. *Colloids and Surfaces A: Physicochemical and Engineering Aspects*, 292(1), 8-20. doi:10.1016/j.colsurfa.2006.05.044
- Kosmatka, S.H., Wilson, M., 2011. *Design and Control of Concrete Mixtures: The Guide to Applications, Methods, and Materials*, 15th Edition.
- Duxson, P., Provis, J. L., Lukey, G. C., & Deventer, J. S., 2007. The role of inorganic polymer technology in the development of ‘green concrete’. *Cement and Concrete Research*, 37(12), 1590-1597. doi:10.1016/j.cemconres.2007.08.018
- Duxson, P., and Provis, J. L., 2008. Designing Precursors for Geopolymer Cements. *Journal of the American Ceramic Society*, 91(12), 3864-3869. doi:10.1111/j.1551-2916.2008.02787.x
- Eijden, J. V., Cornelissen, E., Ruckert, F., & Wolterbeek, T., 2017. Development of Experimental Equipment and Procedures to Evaluate Zonal Isolation and Well Abandonment Materials. *SPE/IADC Drilling Conference and Exhibition*. doi:10.2118/184640-ms
- Enayatpour, S., & Oort, E. V., 2017. Advanced Modeling of Cement Displacement Complexities. *SPE/IADC Drilling Conference and Exhibition*. doi:10.2118/184702-ms
- Fang, G., Bahrami, H., & Zhang, M., 2018. Mechanisms of autogenous shrinkage of alkali-activated fly ash-slag pastes cured at ambient temperature within 24 h. *Construction and Building Materials*, 171, 377-387. doi:10.1016/j.conbuildmat.2018.03.155
- Fernández-Jiménez, A., Monzó, M., Vicent, M., Barba, A., & Palomo, A., 2008. Alkaline activation of metakaolin–fly ash mixtures: Obtain of Zeoceramics and Zeocements. *Microporous and Mesoporous Materials*, 108(1-3), 41-49. doi:10.1016/j.micromeso.2007.03.024

- Geiker, M. Studies of Portland Cement hydration: Measurements of chemical shrinkage and a systematic evaluation of hydration curves by means of the dispersion model (Unpublished doctoral dissertation). Copenhagen.
- Griffith, J., Sabins, F., & Harness, P., 1992. Investigation of Ultrasonic and Sonic Bond Tools for Detection of Gas Channels in Cements. SPE Annual Technical Conference and Exhibition. doi:10.2118/24573-ms
- Hemmings, R. T., & Berry, E. E., 1987. On the Glass in Coal Fly Ashes: Recent Advances. MRS Proceedings, 113. doi:10.1557/proc-113-3
- Juenger, M., Winnefeld, F., Provis, J., & Ideker, J., 2011. Advances in alternative cementitious binders. Cement and Concrete Research, 41(12), 1232-1243. doi:10.1016/j.cemconres.2010.11.012
- Liu, X., 2017. Mud-to-Cement Conversion of Synthetic-Based Drilling Muds Using Geopolymers. PhD Dissertation, the University of Texas at Austin.
- Liu, X., Aughenbaugh, K., Lee, H., et al., 2017. Synthetic Based Mud Hybrid Cements for Primary Cementing and Lost Circulation Control, in: SPE-184558. Presented at the SPE Conference on Oilfield Chemistry, Montgomery, TX.
- Liu, X., Aughenbaugh, K., Nair, S.D., et al., 2016. Solidification of Synthetic-Based Drilling Mud using Geopolymers, in: SPE-180325. Presented at the SPE Deepwater Drilling and Completions Conference, Galveston, TX.
- Ma, Y., Ye, G., 2014 The Shrinkage of alkali activated fly ash. Cement and Concrete Research, 68, 75-82.
- Mehta, P.K and Monteiro, P.J.M, 2006. Concrete: Structure, Properties and Materials, Third Edition, McGraw-Hill.
- Miranda, C.R., Carvalho, K.T., Vargas, A.A., et al., 2007. Minimizing Fluid Contamination during Oilwell Cementing Operations. Presented at the Offshore Mediterranean Conference and Exhibition, Offshore Mediterranean Conference.
- Neto, A. A., Cincotto, M. A., & Repette, W., 2008. Drying and autogenous shrinkage of pastes and mortars with activated slag cement. Cement and Concrete Research, 38 (4), 565-574. doi:10.1016/j.cemconres.2007.11.002
- Parts List and Drawings. (n.d.). Retrieved April 1, 2019, from <https://www.accumulators.com/diaphragm-accumulators/parts-list-drawings/#1494941747215-d4489cc4-212b>
- Pang, X., Bentz, D. P., Meyer, C., Funkhouser, G. P., & Darbe, R., 2013. A comparison study of Portland cement hydration kinetics as measured by chemical shrinkage and isothermal calorimetry. Cement and Concrete Composites, 39, 23-32. doi:10.1016/j.cemconcomp.2013.03.007

- Powers, T.C., 1935. Absorption of Water by Portland Cement Paste during the Hardening Process,” *Industrial and Engineering Chemistry*, Vol. 27, No. 7, pages 790 to 794.
- Provis, J.L., van Deventer, J.S.J., 2014. *Alkali Activated Materials*, RILEM State of-the-Art Reports. Springer Netherlands, Dordrecht.
- Provis, J. L., & Deventer, J. S., 2009. *Geopolymers: Structures, Processing, Properties and Industrial Applications*. Elsevier. doi:10.1533/9781845696382
- Radlinska, A., Rajabipour, F., Bucher, B., Henkensiefken, R., Sant, G., & Weiss, J., 2008. Shrinkage Mitigation Strategies in Cementitious Systems. *Transportation Research Record: Journal of the Transportation Research Board*, 2070(1), 59-67. doi:10.3141/2070-08
- Sant, G., Lura, P., & Weiss, J., 2006. Measurement of Volume Change in Cementitious Materials at Early Ages. *Transportation Research Record: Journal of the Transportation Research Board*, 1979(1), 21-29. doi:10.1177/0361198106197900104
- Singh, G.V.P., Subramaniam, K., 2019. Influence of processing temperature on the reaction product and strength gain in alkali-activated fly ash. *Cement and Concrete Composites*.
- Somna, K., Jaturapitakkul, C., Kajitvichyanukul, P., & Chindaprasirt, P., 2011. NaOH-activated ground fly ash geopolymer cured at ambient temperature. *Fuel*, 90(6), 2118-2124. doi:10.1016/j.fuel.2011.01.018
- Soucy, K., Cramer, B., McDonald, M., et al., 2017. Novel Application of Elemental Aluminum and Zinc to Generate a Self-Compressing Silicate System for Use in Lost Circulation and Conformance, in SPE-187424. Presented at the SPE Annual Technical Conference and Exhibition, San Antonio, 2017.
- Sun, Z., & Vollpracht, A., 2018. Isothermal calorimetry and in-situ XRD study of the NaOH activated fly ash, metakaolin and slag. *Cement and Concrete Research*, 103, 110-122. doi:10.1016/j.cemconres.2017.10.004
- Thomas, J.J., Allen, A.J., Jennings, H.M, 2012. Density and water content of nanoscale solid C–S–H formed in alkali-activated slag (AAS) paste and implications for chemical shrinkage. *Cement and Concrete Research*. 42 (2), 377–383.
- Yong, C.Z., 2010. *Shrinkage Behaviour of geopolymers*. M.Eng.Sci. thesis, University of Melbourne.
- Yusuf, M. O., Johari, M. A., Ahmad, Z. A., & Maslehuddin, M., 2014. Shrinkage and strength of alkaline activated ground steel slag/ultrafine palm oil fuel ash pastes and mortars. *Materials & Design*, 63, 710-718. doi:10.1016/j.matdes.2014.06.062